INSTITUTO POLITÉCNICO DE BRAGANÇA
Escola Superior de Tecnologia e Gestão

The Cation Specific Effects on the Aqueous Solubility of Amino Acids: Experimental and Molecular Dynamics Simulations Contributions

Cátia Sofia Ribeiro De Sousa

Escola Superior de Tecnologia e de Gestão

Instituto Politécnico de Bragança

Master's degree in chemical engineering

July 2014

The Cation Specific Effects on the Aqueous Solubility of Amino Acids: Experimental and Molecular Dynamics Simulations Contributions

Cátia Sofia Ribeiro De Sousa

Escola Superior de Tecnologia e de Gestão

Instituto Politécnico de Bragança

Master's degree in chemical engineering

Supervisors:

Dr. Luciana Tomé

Professor Olga Ferreira

Professor Simão Pinho

July 2014

To my Father.

Acknowledgements

I would like to express my gratitude to my supervisors Professor Simão Pinho and Professor Olga Ferreira for the opportunity to integrate this research project, the possibility of collaboration with CICECO Laboratory at the University of Aveiro, the scientific guidance, and the overall support during the research project.

This work would not be possible without the help of Dr. Luciana Tomé. I am grateful for the scientific guidance, and for her patience and kindness that she showed guiding my research activities.

My grateful acknowledge to Escola Superior de Tecnologia e Gestão (ESTiG) directed by Professor Albano Alves for providing the laboratory space and equipment needed.

I am very grateful to Professor João Coutinho for providing the laboratory space and equipment needed, as well as his support during the research project.

I thank my Path and LSRE/IPB colleagues for the companionship and cooperation.

Finally, special thanks to all those who have been part of my life, for all the affection, dedication and encouragement. Thanks to my Mother and to Lino Maia.

Resumo

O estudo dos efeitos específicos dos iões na solubilidade de aminoácidos e proteínas, em soluções aquosas, é vital para o desenvolvimento de muitas áreas da bioquímica e da biotecnologia.

Neste trabalho estudou-se o efeito dos iões de sais inorgânicos na solubilidade de aminoácidos, em soluções aquosas salinas, através de medições experimentais e simulações de dinâmica molecular. Foram selecionados três aminoácidos (DL-alanina, L-isoleucina e L-valina) como compostos modelo. Face à sua relevância biológica e escassa informação disponível na literatura, selecionaram-se ainda os seguintes catiões: K^+, Li^+, Ca^{2+} e Al^{3+}, variando o anião entre Cl^- ou SO_4^{2-}.

Recorrendo a um método analítico isotérmico mediu-se a solubilidade, a 298,15 K, da DL-alanina (Ala) em soluções aquosas contendo $CaCl_2$ e K_2SO_4 e da L-isoleucina (Iso) e L-valina (Val), em soluções aquosas contendo $CaCl_2$, K_2SO_4, LiCl, Li_2SO_4, $Al_2(SO_4)_3$ e $AlCl_3$. No caso de LiCl, o efeito observado na solubilidade de Val e Iso é praticamente inexistente enquanto Li_2SO_4 e K_2SO_4 induzem um efeito de *salting-out*. Por último, para $CaCl_2$, $Al_2(SO_4)_3$ e $AlCl_3$ observou-se um efeito de *salting-in* bastante pronunciado, sendo mais forte no caso dos sais que contêm alumínio.

Os resultados obtidos pelas simulações de dinâmica molecular sugerem que o efeito de *salting-in* na solubilidade é diferente entre catiões e aniões. Os catiões polivalentes fortemente hidratados (Ca^{2+} e Al^{3+}) apresentam interações extremamente fortes com o grupo carboxílico dos aminoácidos, resultando num efeito pronunciado de *salting-in*. Por outro lado, os iões Li^+ e K^+ não estabelecem interações relevantes com os aminoácidos, apresentando pouco efeito na solubilidade.

Palavras-chave: aminoácidos, solubilidade, efeito de iões, dinâmica molecular

Abstract

The study of ion specific effects on the aqueous solubility of amino acids and proteins is crucial for the development of many areas of biochemistry and biotechnology.

In this work, the effect of ions of inorganic salts on the aqueous solubility of amino acids was studied by performing experimental solubility measurements and molecular dynamics simulations. Three amino acids (DL-alanine, L-isoleucine and L-valine) were chosen as model compounds. Taking into consideration their biological relevance and scarce available information, cations such as K^+, Li^+, $Ca^{2+}$and Al^{3+} were selected, varying the anion between Cl^- or SO_4^{2-}.

New solubility data were measured, at 298.15 K, using the analytical isothermal shake-flask method, for DL-alanine (Ala) in aqueous solutions of $CaCl_2$ and K_2SO_4, and for L-isoleucine (Ile) and L-valine (Val) in aqueous solutions of $CaCl_2$, K_2SO_4, LiCl, Li_2SO_4, $Al_2(SO_4)_3$ and $AlCl_3$. For LiCl no significant solubility effect was observed for Val and Ile while Li_2SO_4 and K_2SO_4 induced a *salting-out* effect. In the case of $CaCl_2$, $Al_2(SO_4)_3$ and $AlCl_3$, a pronounced *salting-in* was observed, much stronger for the aluminum salts.

The molecular dynamics simulations results obtained suggest that the solubility effects of *salting-in* inducing cations is different from that of the anions. Strongly hydrated polyvalent cations (Ca^{2+} and Al^{3+}) present extremely strong interactions with the carboxylic group of the amino acids, resulting in a pronounced *salting-in* effect. On the other hand, Li^+ and K^+ ions do not establish important interactions with the amino acids, having thus a small effect on their aqueous solubility.

Keywords: amino acids, solubility, ion effects, molecular dynamics

Table of Contents

List of Figures ix

List of Tables xv

Chapter 1. Introduction 1

1.1. Motivation and objectives 1

1.2. Structure of the thesis 1

1.3. State of the art 2

1.3.1. The salt effect on the solubility of amino acids and proteins in water 2

1.3.2. Experimental solubility database 5

Chapter 2. Experimental part 13

2.1. Materials and Methods 13

2.1.1. Chemical compounds 13

2.1.2. Experimental procedure 14

2.2. Results and discussion 17

2.2.1. Solubility in water 17

2.2.2. Solubility in aqueous saline solutions 17

2.2.3. pH measurements 22

Chapter 3. Molecular Dynamics Simulation 23

3.1. Introduction 23

3.2. Computational method 25

3.3. Results and discussion 26

3.3.1. Anion effect 28

3.3.2. Cation effect 33

3.3.3. Interactions with water 42

3.3.4. Amino acid side chain effect 45

3.3.4.1. Anions 45
3.3.4.2. Cations 46
Chapter 4. Conclusions and Future Work 49
References 51
Appendix A 57

List of Figures

Figure 1 - Typical order of cations and anions in the Hofmeister series (adapted from Kunz, 2010).....2
Figure 2 - Relative solubility of DL-alanine in aqueous saline solutions, at 298.15 K, containing: ◊, NaF (El-Dossoki 2010); ■, KF (El-Dossoki 2010). 6
Figure 3 - Relative solubility of DL-alanine in aqueous saline solutions, at 298.15 K, containing: ♦, NaBr (El-Dossoki 2010); +, KBr (El-Dossoki 2010).....6
Figure 4 - Relative solubility of DL-alanine in aqueous saline solutions, at 298.15 K, containing: ▲, K_2SO_4 (El-Dossoki 2010); Δ, $(NH_4)_2SO_4$ (Ferreira *et al.* 2009). 7
Figure 5 - Relative solubility of DL-alanine in aqueous saline solutions, at 298.15 K, containing: Δ, KCl (Khoshkbarchi and Vera 1997); ○, KCl (Ferreira *et al.* 2005); □, $CaCl_2$ (El-Dossoki 2010); □, NH_4Cl (Tomé *et al.* 2013); ×, NaCl (Khoshkbarchi and Vera 1997); ●, $BaCl_2$ (El-Dossoki 2010). 7
Figure 6 - Relative solubility of L-valine in aqueous solutions, at 298.15 K, containing: ◊, NaF (El-Dossoki 2010); ■, KF (El-Dossoki 2010). 8
Figure 7 - Relative solubility of L-valine in aqueous solutions, at 298.15 K, containing: ♦, NaBr (El-Dossoki 2010); +, KBr (El-Dossoki 2010). 8
Figure 8 - Relative solubility of L-valine in aqueous solutions containing, at 298.15 K,: □, $CaCl_2$ (El-Dossoki 2010); ●, $BaCl_2$ (El-Dossoki 2010); □, NH_4Cl (Tomé *et al.* 2013); ○, $MgCl_2$ (Tomé *et al.* 2013).....9
Figure 9 - Relative solubility of L-valine in aqueous solutions, at 298.15 K, containing: ▲, K_2SO_4 (El-Dossoki 2010); ▲, $(NH_4)_2SO_4$ (Tomé *et al.* 2013); ◊, $MgSO_4$ (Tomé *et al.* 2013).....9
Figure 10 - Relative solubility of L-valine in aqueous solutions, at 298.15 K, containing: ×, Na_2SO_4 (El-Dossoki 2010); ×, Na_2SO_4 (Ramasami 2002); ×, Na_2SO_4 (Islam and Wadi 2001)....10
Figure 11 - Relative solubility of L-isoleucine in aqueous solutions, at 298.15 K, containing: Δ, $(NH_4)_2SO_4$ (Ferreira *et al.* 2009); ◊,$MgSO_4$ (Tomé *et al.* 2013). 10
Figure 12 - Relative solubility of L-isoleucine in aqueous solutions, at 298.15 K, containing: □, KCl (Ferreira *et al.* 2007); □, NH_4Cl (Tomé *et al.* 2013); ○, $MgCl_2$ (Tomé *et al.* 2013). 11
Figure 13 - Structure of the amino acids studied in this work: (a) alanine, (b) valine and (c) isoleucine.....13

Figure 14 - Experimental setup used on the shake flask method. 14
Figure 15 - Density meter used in this work. 15
Figure 16 - Typical refractive index versus concentration of amino acid curve, obtained by applying method B. 16
Figure 17 – Refractometer used in this work. 16
Figure 18 - Relative solubility of alanine (blue), valine (red), and isoleucine (green) in aqueous solutions, at 298.15 K, containing the salt: (a) □, LiCl; Δ, $CaCl_2$; and in (b) ◊, Li_2SO_4; ○, K_2SO_4. Lines are guides to the eyes. 20
Figure 19 - Relative solubility of DL-alanine in potassium sulfate aqueous solutions obtained in this work and by El-Dossoki (2010), at 298.15 K. 21
Figure 20 - Relative solubility of DL-alanine in $CaCl_2$ aqueous solutions obtained in this work and by El-Dossoki (2010), at 298.15 K. 21
Figure 21 - Structure and atom labeling of the amino acids studied in this work: (a) alanine (Ala), (b) valine (Val) and (c) isoleucine (Ile). C_t stands for the terminal carbon atom of the amino acid side chain and C_B is used to denote the carbon backbone of the amino acid side chain. 27
Figure 22 - Radial distribution functions corresponding to the interactions of isoleucine C_t with the central atom of the anions (Cl or S), for salts containing Li^+ and Al^{3+} cations. 28
Figure 23 - Radial distribution functions corresponding to the interactions of isoleucine C_B with the central atom of the anions (Cl or S), for salts containing Li^+ and Al^{3+} cations. 29
Figure 24 - Radial distribution functions corresponding to the interactions of the H atom of the amine group of isoleucine with the central atom of the anions (Cl or S), for salts containing Li^+ and Al^{3+} cations. 29
Figure 25 - Radial distribution functions corresponding to the interactions of the O atom of the carboxylic group of isoleucine with the central atom of the anions (Cl or S), for salts containing Li^+ and Al^{3+} cations. 30
Figure 26 - Radial distribution functions corresponding to the interactions of Li_2SO_4 salts with water molecules, in the presence of isoleucine. 33
Figure 27 - Radial distribution functions corresponding to the interactions of isoleucine C_t with the cations (Li^+, K^+, Ca^{2+} or Al^{3+}) for all the studied salts. 34
Figure 28 - Radial distribution functions corresponding to the interactions of isoleucine C_B with the cations (Li^+, K^+, Ca^{2+} or Al^{3+}) for all the studied salts. 34

Figure 29 - Radial distribution functions corresponding to the interactions of the O atom of the carboxylic group of isoleucine with the monovalent cations (Li^+ or K^+) for all the studied salts. 35
Figure 30 - Radial distribution functions corresponding to the interactions of the O atom of the carboxylic group of isoleucine with the polyvalent cations (Ca^{2+} or Al^{3+}) for all the studied salts. 35
Figure 31 – Snapshot from a simulation of (Ile + LiCl + water) mixtures, showing the distances (Å) between selected atoms. Light blue spheres represent carbon atoms, dark blue spheres are nitrogen atoms, red spheres are oxygen, white spheres are hydrogen, green spheres are chloride and pink spheres are lithium. Water molecules are represented in line style.....37
Figure 32 - Snapshot from a simulation of (Ile + Li_2SO_4 + water) mixtures, showing the distances (Å) between selected atoms. Light blue spheres represent carbon atoms, dark blue spheres are nitrogen atoms, red spheres are oxygen, white spheres are hydrogen, yellow spheres are sulfur and pink spheres are lithium. Water molecules are represented in line style.....37
Figure 33 - Snapshot from a simulation of (Ile + $AlCl_3$ + water) mixtures, showing the distances (Å) between selected atoms. Light blue spheres represent carbon atoms, dark blue spheres are nitrogen atoms, red spheres are oxygen, white spheres are hydrogen, green spheres are chloride and orange spheres are aluminum. Water molecules are represented in line style. 38
Figure 34 - Snapshot from a simulation of (Ile + $Al_2(SO_4)_3$ + water) mixtures, showing the distances (Å) between selected atoms. Light blue spheres represent carbon atoms, dark blue spheres are nitrogen atoms, red spheres are oxygen, white spheres are hydrogen, yellow spheres are sulfur and orange spheres are aluminum. Water molecules are represented in line style. 38
Figure 35 - Radial distribution function for the interactions between water molecules and the ions in aqueous solutions of Ile in the presence of $Al_2(SO_4)_3$. 41
Figure 36 - Radial distribution functions corresponding to the interaction of isoleucine C_t with water molecules, in the presence of all the studied salts. 43
Figure 37 - Radial distribution functions corresponding to the interaction of the H atom of the amine group of isoleucine with water molecules, in the presence of all the studied salts. 43
Figure 38 - Radial distribution functions corresponding to the interaction of the O atom of the carboxylic group of isoleucine with water molecules, in the presence of all the studied salts. 44

Figure 39 - Radial distribution functions corresponding to the interaction of the terminal carbon atom of all the amino acids studied with the central atom of the anion for aqueous solutions of Li_2SO_4.....46
Figure 40 - Radial distribution functions corresponding to the interactions of all the studied amino acids C_t with the cation of $AlCl_3$. 47
Figure 41 - Radial distribution functions corresponding to the interactions of the O atom of the carboxylic group of all the studied amino acids with the cation of $AlCl_3$. 47
Figure A.1 - Radial distribution functions corresponding to the interactions of alanine C_t with the central atom of the anions (Cl or S), for salts containing Li^+ and Al^{3+} cations.....57
Figure A.2 - Radial distribution functions corresponding to the interactions of the H atom of the amine group of alanine with the central atom of the anions (Cl or S), for salts containing Li^+ and Al^{3+} cations.....57
Figure A.3 - Radial distribution functions corresponding to the interactions of the O atom of the carboxylic group of alanine with the central atom of the anions (Cl or S), for salts containing Li^+ and Al^{3+} cations. 58
Figure A.4 - Radial distribution functions corresponding to the interactions of valine C_t with the central atom of the anions (Cl or S), for salts containing Li^+ and Al^{3+} cations.....58
Figure A.5 - Radial distribution functions corresponding to the interactions of the H atom of the amine group of valine with the central atom of the anions (Cl or S), for salts containing Li^+ and Al^{3+} cations.....59
Figure A.6 - Radial distribution functions corresponding to the interactions of the O atom of the carboxylic group of valine with the central atom of the anions (Cl or S), for salts containing Li^+ and Al^{3+} cations. 59
Figure A.7 - Radial distribution functions corresponding to the interactions of alanine Ct with the cations (Li^+, K^+, Ca^{2+} or Al^{3+}) for all the studied salts. 60
Figure A.8 - Radial distribution functions corresponding to the interactions of the O atom of the carboxylic group of alanine with the monovalent cations (Li^+ or K^+) for all the studied salts. 60
Figure A.9 - Radial distribution functions corresponding to the interactions of the O atom of the carboxylic group of alanine with the polyvalent cations (Ca^{2+} or Al^{3+}) for all the studied salts. ..61
Figure A.10 - Radial distribution functions corresponding to the interactions of valine C_t with the cations (Li^+, K^+, Ca^{2+} or Al^{3+}) for all the studied salts. 61

Figure A.11 - Radial distribution functions corresponding to the interactions of valine C_B with the cations (Li^+, K^+, Ca^{2+} or Al^{3+}) for all the studied salts. 62
Figure A.12 - Radial distribution functions corresponding to the interactions of the O atom of the carboxylic group of valine with the monovalent cations (Li^+ or K^+) for all the studied salts. 62
Figure A.13 - Radial distribution functions corresponding to the interactions of the O atom of the carboxylic group of valine with the polyvalent cations (Ca^{2+} or Al^{3+}) for all the studied salts. 63
Figure A.14 - Radial distribution functions corresponding to the interaction of alanine C_t with water molecules, in the presence of all the studied salts. 63
Figure A.15 - Radial distribution functions corresponding to the interaction of the H atom of the amine group of alanine with water molecules, in the presence of all the studied salts. 64
Figure A.16 - Radial distribution functions corresponding to the interaction of the O atom of the carboxylic group of alanine with water molecules, in the presence of all the studied salts. 64
Figure A.17 - Radial distribution functions corresponding to the interaction of valine C_t with water molecules, in the presence of all the studied salts. 65
Figure A.18 - Radial distribution functions corresponding to the interaction of the H atom of the amine group of valine with water molecules, in the presence of all the studied salts. 65
Figure A.19 - Radial distribution functions corresponding to the interaction of the O atom of the carboxylic group of valine with water molecules, in the presence of all the studied salts. 66
Figure A.20 - Radial distribution functions corresponding to the interaction of the terminal carbon atom of all the amino acids studied with the central atom of the anion for aqueous solutions of K_2SO_4. 66
Figure A.21 - Radial distribution functions corresponding to the interaction of the terminal carbon atom of all the amino acids studied with the central atom of the anion for aqueous solutions of $Al_2(SO_4)_3$. 67
Figure A.22 - Radial distribution functions corresponding to the interactions of all the studied amino acids C_t with the cation of $CaCl_2$ 67
Figure A.23 - Radial distribution functions corresponding to the interactions of the O atom of the carboxylic group of all the studied amino acids with the cation of $CaCl_2$. 68

List of Tables

Table 1 – Experimental solubility data of amino acids in aqueous saline solutions published in the literature. 5
Table 2 - Solubility (in molality, mol/kg) of the salts used in this work, in pure water, at 298.15 K (Lide 2003). 13
Table 3 - Source and purity of the chemicals used in this work. 13
Table 4 - Comparison of the solubility of amino acids (g amino acid/1000 g of water) in pure water, at 298.15K. 17
Table 5 - DL-alanine, L-valine and L-isoleucine solubility at 298.15 K in aqueous solutions of K_2SO_4, measured by the experimental method A.1. 18
Table 6 - L-valine and L-isoleucine solubility at 298.15 K in aqueous solutions of LiCl, measured by the experimental method A.2. 18
Table 7 - L-valine and L-isoleucine solubility at 298.15 K in aqueous solutions of Li_2SO_4, measured by the experimental method A.2. 18
Table 8 - DL-alanine, L-valine and L-isoleucine solubility at 298.15 K in aqueous solutions of $CaCl_2$, measured by the experimental method A.2. 18
Table 9 - L-valine and L-isoleucine solubility at 298.15 K in aqueous solutions of $Al_2(SO_4)_3$, measured by the experimental method B. 19
Table 10 - L-valine and L-isoleucine solubility at 298.15 K in aqueous solutions of $AlCl_3$, measured by the experimental method B. 19
Table 11 - pH values measured for amino acids studied in aqueous saline solution at 298 K. 22
Table 12 - Values ($kJmol^{-1}$) of the Lennard-Jones (LJ) and Coulomb (Coul) terms of the energies calculated for the interactions (amino acid-water), (amino acid-anion) and (amino acid-cation) for the different systems under study. 32
Table 13 - Molar entropy of hydration, $\Delta_{hyd}S$, and Gibbs free energy of hydration, $\Delta_{hyd}G$, at 298.15 K (Marcus, 1997). 39

Table A.1 - Position and intensities of the RDF peak maxima corresponding to the interactions of selected group of Ile with the anion (A^{x-}), the cation (B^{y+}), and the oxygen (O_{H2O}) and hydrogen atoms of water (H_{H2O}), for all the systems studied.....69

Chapter 1. Introduction

1.1. Motivation and objectives

The comprehension of the molecular interactions that control vital biochemical processes involving amino acids and proteins in aqueous saline solutions is still a thematic of great interest. In the last years, several molecular mechanisms have been proposed to interpret the Hofmeister series that establishes the anions and cations effects on the aqueous solubility of proteins. Although phenomenologically well established, the mechanisms governing the solubility effects of ions are still poorly understood, in particular as far as the cations are concerned. The lack of a consensual molecular picture of these phenomena has been limiting the development of medical and pharmaceutical solutions to diseases induced by biochemical disorders and the development of biotechnological processes (Tomé *et al.* 2013).

The objective of this work is to give a contribution to the understanding of the effect of the anions and (more particularly) of the cations of inorganic salts on the aqueous solubility of amino acids, using a method combining experimental and simulation techniques. With that aim, following the methodology previously proposed (Tomé *et al.* 2010, Tomé *et al.* 2013), the effect of the nature of the anion, of the cation and of the structure of the amino acid on the aqueous solubility of amino acids was studied by performing both experimental solubility measurements and molecular dynamics (MD) simulations, extending it to new amino acid + salt systems for which scarce information is currently available. DL-alanine, L-isoleucine and L-valine were chosen as model compounds of peptides and proteins, allowing to observe the impact of the alkyl chain. Taking into consideration their differentiated position in the Hofmeister series and expected impact on the solubility, cations such as K^+, Li^+, $Ca^{2+}$and Al^{3+} were selected, varying the anion between Cl^- or SO_4^{2-}.

1.2. Structure of the thesis

In Chapter 1, the fundamental concepts for the study of the salt's effect on the solubility of proteins and amino acids in aqueous solutions are presented, as well as a literature review on the solubility data of the amino acids studied in this work, in aqueous saline solutions. In Chapter 2, the experimental methods and materials for the solubility measurements are detailed and the

correspondent results are presented and discussed. Chapter 3 is dedicated to the molecular dynamics simulations, including the main theoretical concepts, the computational method as well as the presentation of results and discussion. Finally, in Chapter 4, the main conclusions and suggestions for future work are described.

1.3. State of the art

In this section, some fundamental concepts to study the effect of the salts on the solubility of amino acids and proteins in aqueous solutions will be discussed.

1.3.1. The salt effect on the solubility of amino acids and proteins in water

Over time, specific ion effects on biomolecules solubility were identified from the ability of some salts to precipitate proteins in aqueous solutions (Kunz *et al.* 2004). In particular, experimental studies show that the solubility behavior of amino acid in aqueous saline solutions is affected by the nature and concentration of cations and anions, as well as the structural characteristics of biomolecules, pH and temperature (Ramasami 2002, Ferreira *et al.* 2009).

The work from Franz Hofmeister (1888), which focuses on the specific effects of ions, is presented as a reference in this research area. The relative influence of ions on the physical and chemical behavior of aqueous systems was ranked in what is known as the Hofmeister series, illustrated in Figure 1.

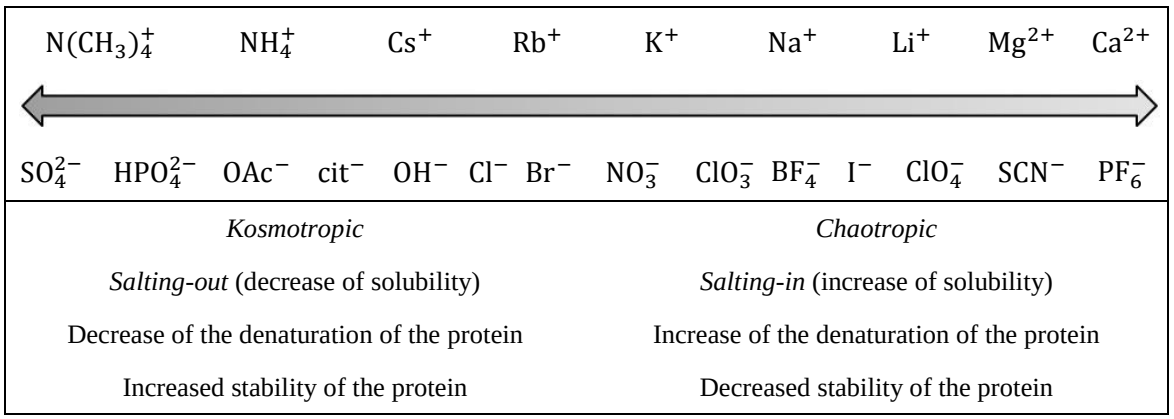

Figure 1 - Typical order of cations and anions in the Hofmeister series (adapted from Kunz, 2010).

A group of salts can be classified according to their efficiency to precipitate proteins, *salting-out*, while another group can be rated according to their efficiency to solubilize proteins, *salting-in* (Collins 2004). The typical order may differ, depending on the system's property that is being examined in which case some ions may change their position in the series (Kunz 2010).

Knowledge of the molecular mechanisms is fundamental to interpret the solubility of amino acids in the presence of salts, and may provide useful information for understanding the behavior of the protein solubility as well as other complex biomolecules (Tomé *et al.* 2010). However, those mechanisms are far from being elucidated and consensual. For some authors, the main cause of the effect was related to how the bulk water structure was affected by ions. *Salting-out* inducing ions, known as "kosmotropes", were believed to be able to create the bulk water structure, precipitating proteins and preventing folding. On the other hand, *salting-in* inducing ions, classified as "chaotropes", would destroy it, promoting the solubilization of folded macromolecules (Tomé *et al.* 2010).

During the last years, significant progress has been made to understand the specific effects of ions. Thus, new ideas have emerged on the origin of those effects and new techniques were developed to study them (Kunz 2010), being the structure maker/breaker classical approach questioned. Even today, to explain or even to predict the relative importance of ion-ion and ion-water interactions is much debated. On one hand, some authors are convinced that a good description of the dispersion forces would be sufficient; others, that the proper description of the geometry of ions or charged head groups and water is crucial (Kunz 2010).

Experimental and simulation studies show that the ions have a small effect on the hydrogen bonding of water in bulk solution. Recently, new theories considering the significant role of dispersion forces, involving the relative polarizabilities of the ions and the specific ion binding have been proposed (Tomé *et al.* 2010).

One of the most consistent theories was proposed by Zhang *et al.* (2005), describing the specific effects of ions on the solubility of macromolecules in water. This theory claims that the Hofmeister effects of salts on the solubilities of macromolecules depend on direct interactions between ions and macromolecules and with water molecules in the first hydration shell of the solutes.

Amino acids are the simplest building blocks of more complex biomolecules, such as proteins, being ideal molecules to be studied as model compounds. Taking this into account,

recently, the theory of Zhang was successfully extended to the interpretation of the cation and anion specific effects on the aqueous solubility of amino acids (Tomé *et al.* 2010, Tomé *et al.* 2013), using MD simulations. With these simulations, it has been possible to achieve a better understanding of the molecular phenomena behind the *salting-in* and *salting-out* effects of salts, by analyzing the presence or absence of interactions between the various chemical species present in the systems (Tomé *et al.* 2013).

According to the conventional model, which designates ions as *kosmotropic* and *chaotropic*, the observed salt effects on the solubility of amino acids are due to changes in the structure of water. Results obtained by MD simulations indicate that the structure of water and the water solvation of amino acids is not significantly affected by the presence of salts. In the presence of an ion with high charge density and strongly hydrated, as in the case of the SO_4^{2-}anion, the solubility of the studied amino acids (DL-alanine, L-isoleucine and L-valine) decreases. Results obtained by MD simulations show preferential binding to the charged moieties of the amino acids and practically no interaction with their non-polar groups (Tomé *et al.* 2010). In contrast, it appears that large and weakly hydrated anions (such as ClO_4^-) interact directly with the non-polar parts of the amino acids, promote its stabilization in water and, consequently, induce *salting-in* effects.

In the case of anions positioned in the middle of the Hofmeister series, such as the anion Cl^-, there is no significant effect on the aqueous solubility of the amino acids as the ion establishes weak interactions with the amino acid. The NO_3^- anion seems to be able to establish more important interactions with hydrophobic and hydrophilic portions of the solute, thus, affecting more markedly its solubility.

As far as cations are concerned, the simulation evidence suggests that due to its high charge density, Mg^{2+} is able to form charged complexes with the amino acids, especially with the negatively charged carboxyl group, promoting a strong *salting-in*. The association of Mg^{2+} with the amino acids is much more remarkable than that of others cations, such as, Na^+, K^+ or even NH_4^+ (Tomé *et al.* 2013).

1.3.2. Experimental solubility database

Table 1 shows a literature review of the solubility data of the amino acids studied in this work (alanine, isoleucine and valine), in aqueous solutions containing salts, published until May 2014. As can be seen, a few data can be found for systems containing K_2SO_4 and $CaCl_2$; however, to our knowledge, no data was published for salts containing either aluminum or lithium cations.

Table 1 – Experimental solubility data of amino acids in aqueous saline solutions published in the literature.

References	Amino acids (purity)	Temperature	Salts (range of molality)
Ferreira *et al.* (2009)	DL-alanine (99%) L-isoleucine (99%)	298.15 and 323.15 K	$(NH_4)_2SO_4$ (0 - 2 molal)
Ferreira *et al.* (2007)	DL-alanine (99%) L-isoleucine (99%)	DL-alanine at 323.15K L-isoleucine at 298.15K and 323.15K	KCl (0 - 2 molal)
Ferreira *et al.* (2005)	DL-alanine (99%)	298.15K	KCl (0 - 2 molal) Na_2SO_4 (0 - 2 molal)
Ramasami (2002)	DL-alanine (99%) DL-valine (99%)	288.15K 298.15K 308.15K	Na_2SO_4 (0.5 - 1.5 molal)
Islam and Wadi (2001)	DL-alanine (99%) DL-valine (99%)	288.15K 298.15K 308.15K	Na_2SO_4 (0.5 - 1 molal)
(Pradhan and Vera 1998)	DL-alanine (99%)	298.2K	NaOH (0 - 8 molal) KOH (0 - 8 molal)
(Pradhan and Vera 2000)	DL-alanine (99%) DL-valine (99%)	298.15K	$NaNO_3$ (0 - 1.5 molal) KNO_3 (0 - 1.5 molal)
(El-Dossoki 2010)	DL-alanine (99%) DL-valine (99%)	298.15K	NaF; KF; NaBr; KBr; NaI; KI; Na_2SO_4; K_2SO_4; $CaCl_2$; $BaCl_2$ (0 - 1 molal)
(Tomé *et al.* 2013)	DL-alanine(99%) DL-valine(99%) L-isoleucine(99%)	298.15K	NH_4Cl; $(NH_4)_2SO_4$; $MgCl_2$; $MgSO_4$ (0 - 2 molal)

Figures 2-12 show the relative solubility of the three amino acids under study (DL-alanine, L-valine and L-isoleucine, respectively), as a function of the salt's molality. The relative

solubility is defined as the ratio of the solubility of the amino acid solution containing the electrolyte, *S*, and the solubility of the amino acid in pure water, S_0. For comparative purposes, the solubility data of salts containing the same anion are presented in the same figure.

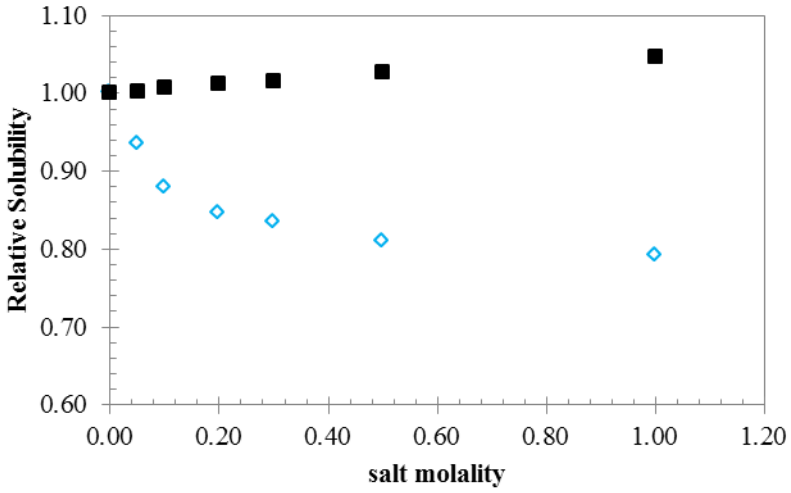

Figure 2 - Relative solubility of DL-alanine in aqueous saline solutions, at 298.15 K, containing: ◊, NaF (El-Dossoki 2010); ■, KF (El-Dossoki 2010).

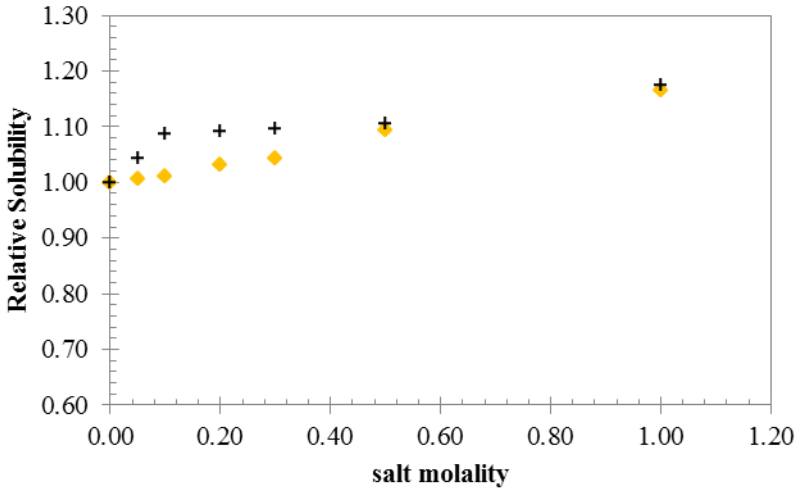

Figure 3 - Relative solubility of DL-alanine in aqueous saline solutions, at 298.15 K, containing: ♦, NaBr (El-Dossoki 2010); +, KBr (El-Dossoki 2010).

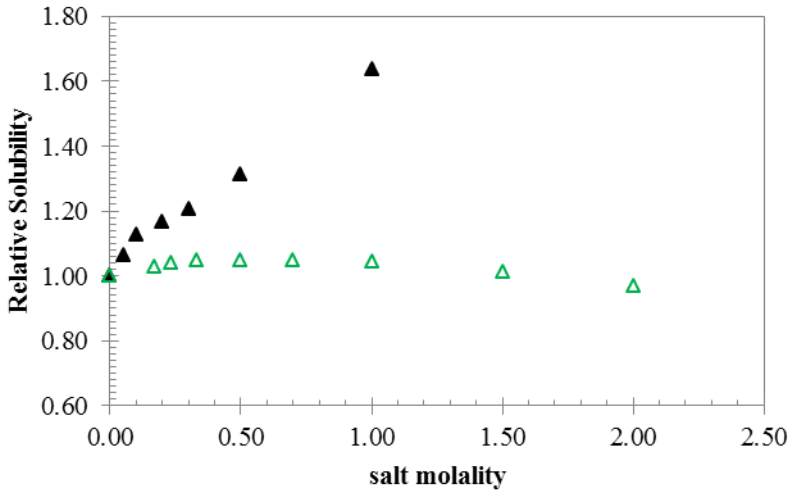

Figure 4 - Relative solubility of DL-alanine in aqueous saline solutions, at 298.15 K, containing: ▲, K_2SO_4 (El-Dossoki 2010); Δ, $(NH_4)_2SO_4$ (Ferreira *et al.* 2009).

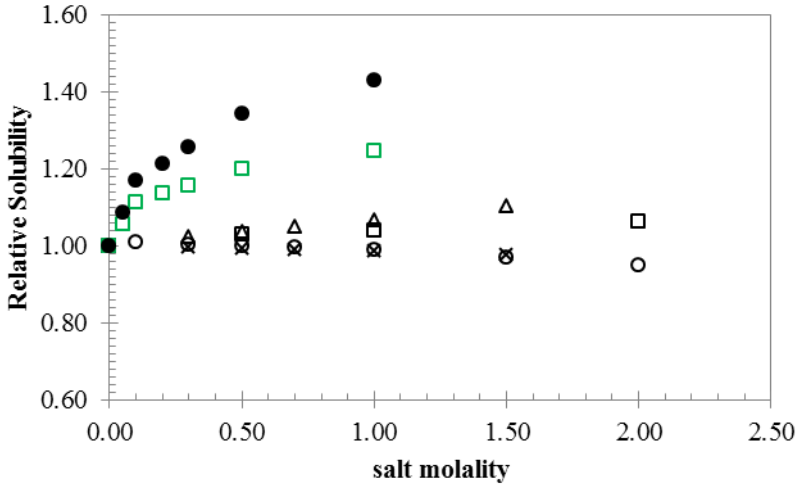

Figure 5 - Relative solubility of DL-alanine in aqueous saline solutions, at 298.15 K, containing: Δ, KCl (Khoshkbarchi and Vera 1997); ○, KCl (Ferreira *et al.* 2005); □, $CaCl_2$ (El-Dossoki 2010); □, NH_4Cl (Tomé *et al.* 2013); ×, NaCl (Khoshkbarchi and Vera 1997); ●, $BaCl_2$ (El-Dossoki 2010).

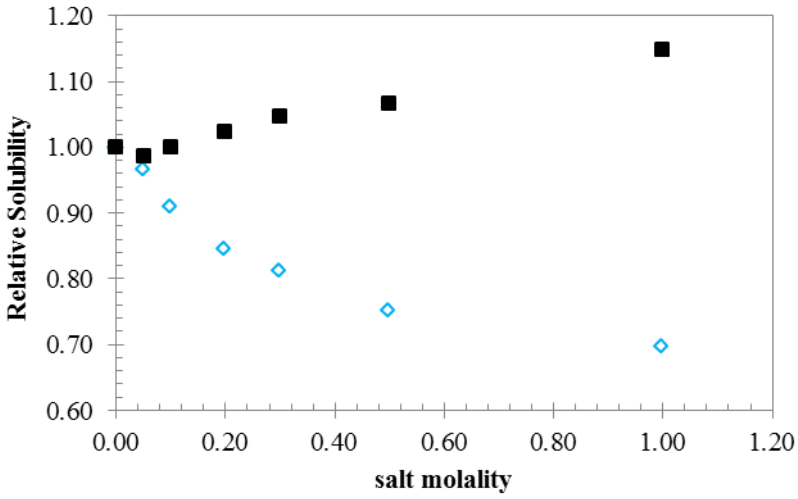

Figure 6 - Relative solubility of L-valine in aqueous solutions, at 298.15 K, containing: ◊, NaF (El-Dossoki 2010); ■, KF (El-Dossoki 2010).

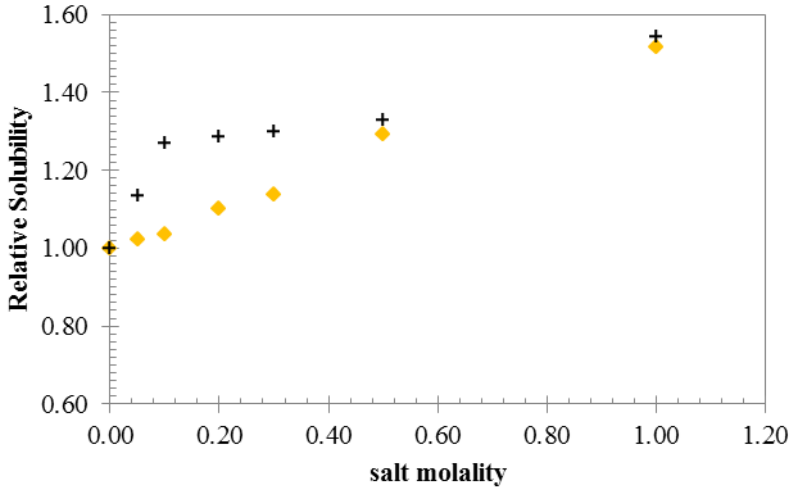

Figure 7 - Relative solubility of L-valine in aqueous solutions, at 298.15 K, containing: ♦, NaBr (El-Dossoki 2010); +, KBr (El-Dossoki 2010).

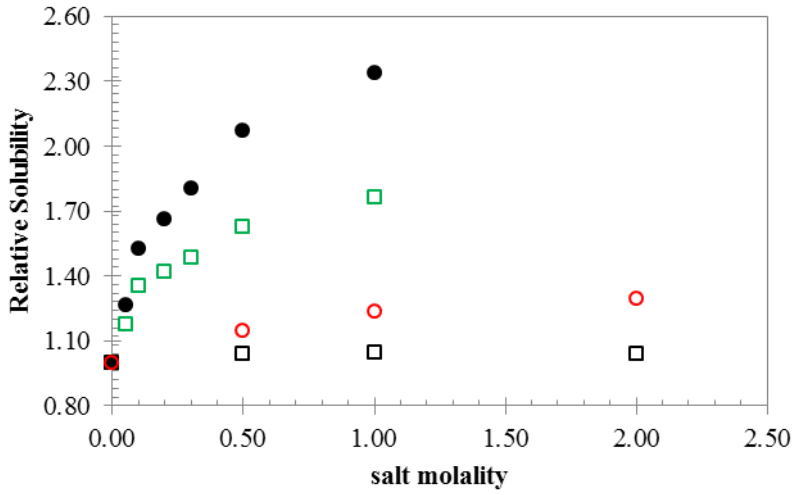

Figure 8 - Relative solubility of L-valine in aqueous solutions containing, at 298.15 K,: □, $CaCl_2$ (El-Dossoki 2010); ●, $BaCl_2$ (El-Dossoki 2010); □, NH_4Cl (Tomé *et al.* 2013); ○, $MgCl_2$ (Tomé *et al.* 2013).

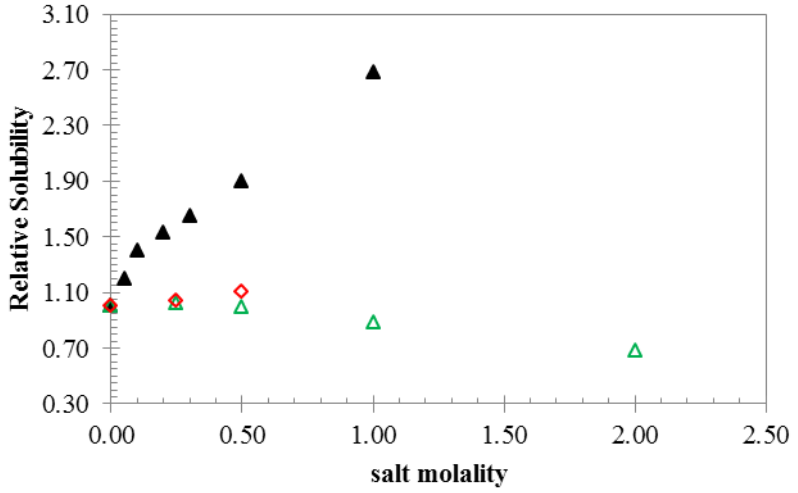

Figure 9 - Relative solubility of L-valine in aqueous solutions, at 298.15 K, containing: ▲, K_2SO_4 (El-Dossoki 2010); ▲, $(NH_4)_2SO_4$ (Tomé *et al.* 2013); ◊, $MgSO_4$ (Tomé *et al.* 2013).

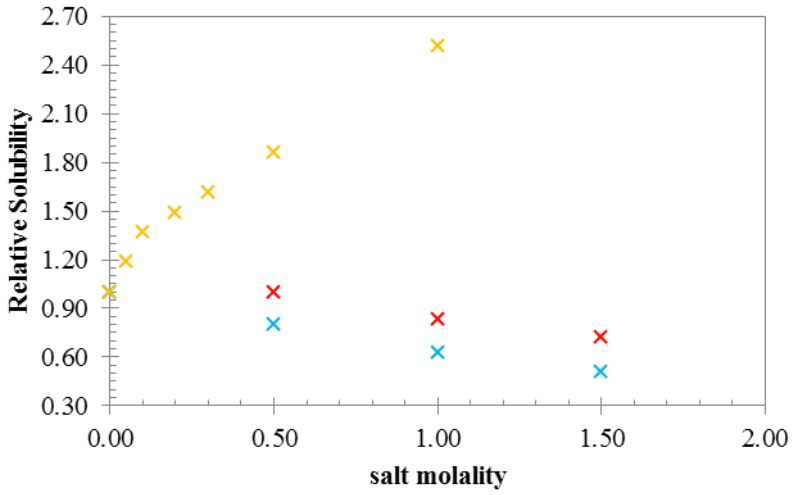

Figure 10 - Relative solubility of L-valine in aqueous solutions, at 298.15 K, containing: ×, Na_2SO_4 (El-Dossoki 2010); ×, Na_2SO_4 (Ramasami 2002); ×, Na_2SO_4 (Islam and Wadi 2001).

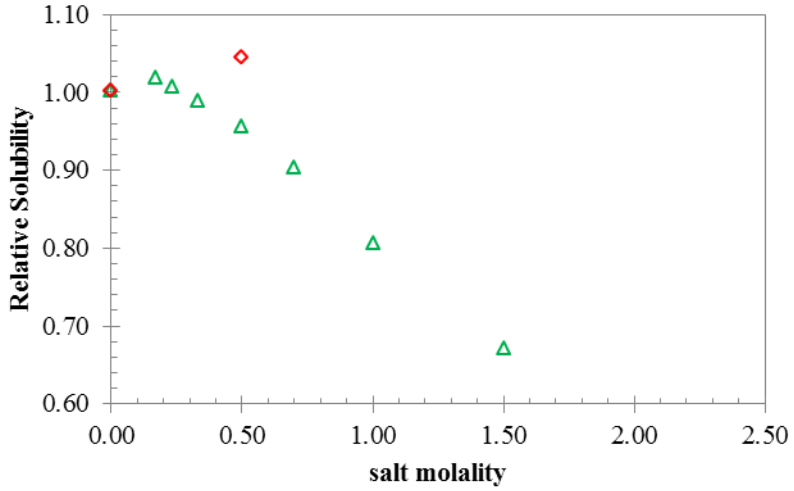

Figure 11 - Relative solubility of L-isoleucine in aqueous solutions, at 298.15 K, containing: Δ, $(NH_4)_2SO_4$ (Ferreira *et al.* 2009); ◊,$MgSO_4$ (Tomé *et al.* 2013).

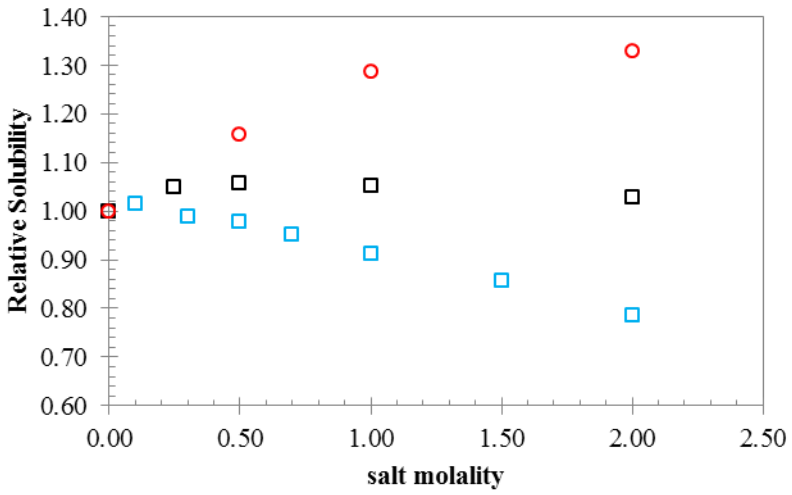

Figure 12 - Relative solubility of L-isoleucine in aqueous solutions, at 298.15 K, containing: □, KCl (Ferreira *et al.* 2007); □, NH_4Cl (Tomé *et al.* 2013); ○, $MgCl_2$ (Tomé *et al.* 2013).

As can be seen in Figures 2-5, some results in literature are contradictory and/or not expected. For example, according to the data represented in Figure 4, s*alting-in* induced by K_2SO_4 was observed. However, that is not very likely to occur for DL-alanine. In fact, $SO_4^{2-}$is a strong *salting-out* inducing anion, an effect that should prevail in the presence of a cation such as K^+, with little effect in the solubility (Tomé *et al.* 2013). Relatively to $(NH_4)_2SO_4$, a slight *salting-in* effect was observed only at lower concentrations, followed by an expected *salting-out* effect.

Figure 5 compares the experimental results for DL-alanine in different salt solutions containing the chloride anion. According to Khoshkbarchi and Vera (1997), the electrolyte KCl induces a *salting-in* effect; however, according to the results reported by Ferreira *et al.* (2005), the situation only occurs at low concentrations of electrolyte. For higher concentrations, *salting-out* is observed. In either situation, however, Ferreira *et al.* (2005) observed less pronounced effects of KCl on the solubility of the amino acid, as would be expected for this salt, positioned in the middle of the Hofmeister series.

In case of Figure 10, the results presented are contradictory. The results obtained by Islam and Wadi (2001) and Ramasami (2002) show that Na_2SO_4 induces a *salting-out* effect, as expected because SO_4^{2-} should behave as a strong *salting-out* inducing anion. However, the results obtained by El-Dossoki (2010) show that Na_2SO_4 induces a *salting-in* effect.

As shown in Figure 5, Figure 8 and Figure 12, either $CaCl_2$ or $MgCl_2$ salts induce a strong *salting-in* effect for DL-alanine, L-valine and L-isoleucine as it would be expected in the case of salts formed by a strong *salting-in* cation and an anion positioned in the middle of the Hofmeister series.

Chapter 2. Experimental part

2.1. Materials and Methods

2.1.1. Chemical compounds

The structure of the three amino acids studied in this work is illustrated in Figure 13.

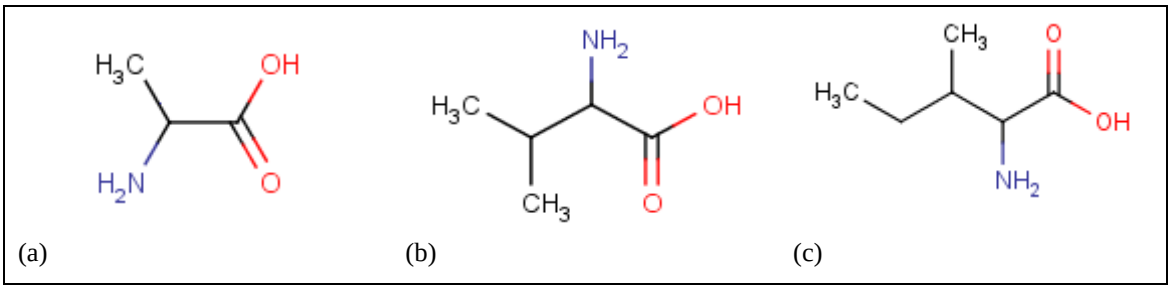

Figure 13 - Structure of the amino acids studied in this work: (a) alanine, (b) valine and (c) isoleucine.

Table 2 shows the solubility in water (mol/kg) of each of the salts to be used in this work. The source and purity of the chemicals are presented in Table 3.

Table 2 - Solubility (in molality, mol/kg) of the salts used in this work, in pure water, at 298.15 K (Lide 2003).

Cation / Anion	Li^+	Ca^{2+}	Mg^{2+}	Al^{3+}	K^+
Cl^-	19.9288	7.3218	5.8825	3.3853	4.7670
SO_4^{2-}	3.1117	0.0151	2.9646	1.1253	0.6876

Table 3 - Source and purity of the chemicals used in this work.

Chemical name	Supplier	Mass fraction purity (%)
DL-Alanine	Merck	≥ 99.0
L-Valine	Merck	≥ 99.0
L-Isoleucine	Merck, Fluka	≥ 99.0
Lithium chloride	Merck	≥ 99.0
Lithium sulfate monohydrate	Merck	≥ 99.0
Calcium chloride dehydrate	Merck	99.0-102.0
Potassium sulfate	Panreac	≥ 99.0
Aluminum chloride hexahydrate	Merck	97.0-101.0
Aluminum sulfate octadecahydrate	VWR CHEMICALS	53.4 (anhydrous basis)

2.1.2. Experimental procedure

Two experimental methods, based on the shake flask method, were used to measure the solubility of amino acids in aqueous saline solutions: method A, described by Tomé *et al.* (2013) and method B, adapted from the work of Venkatesu *et al.* (2006). Both will be described next.

Method A

- Saturated solutions were prepared by mixing a small excess of solid solute with 80 cm^3 of solvent, by previously weighing (±0.1 mg) appropriate amounts of salt and water.
- In order to attain equilibrium, the solution was continuously stirred for 48 hours and, after this period, stirring was stopped. In the following 12 h, the solution was kept at rest. In this process, the temperature was monitored by means of two platinum wires (Pt-104, Pico Technology) in direct contact with the solutions. This system was calibrated, ensuring that the temperature of the solution was between ±0.1 K of the set temperature. Figure 14 shows an image of the experimental setup.

Figure 14 - Experimental setup used on the shake flask method.

- Samples (5 cm^3) of the saturated liquid phase were collected using plastic syringes and polypropylene filters (0.45 μm) previously heated to avoid precipitation of the amino acid.
- Depending on the salt, two different methods for quantitative analysis were chosen: gravimetry, for the anhydrous salts and densimetry for the hydrated salts. Both methods of analysis will be described.

A.1 Gravimetry

- The sample was placed into pre-weighed glass vessels and weighed;
- In order to completely dry the crystals, it is necessary to remove all the solvent present in the sample.
- First, the sample was gently dried in a heating plate for 3-5 days;
- Then, the sample was placed in a drying stove at 343.15 K for at least 3 days;
- Finally, the glass vessels were cooled in the dehydrator with silica gel for several hours and then weighed;
- The last two steps were repeated until the weight remained constant, in two consecutive weekly measurements. Each solubility value was an average of at least three different measurements.

A.2 Densimetry

Densities were measured using a vibrating tube digital density meter (DMA 5000 M, Anton Paar), shown in Figure 15, with a reproducibility within $\pm 3 \times 10^{-3}$ kg/m^3.

Figure 15 - Density meter used in this work.

- For each amino acid and salt molality, a linear calibration curve density *vs* concentration of amino acid was determined. For this, 6 standards were prepared and the correspondent density measured.

Method B

- For a given salt molality, about 12 vials were prepared by adding different amounts of amino acid. The weighed samples were prepared so that at least six samples would result in saturated solutions and, the remaining would be unsaturated, as illustrated in Figure 16.

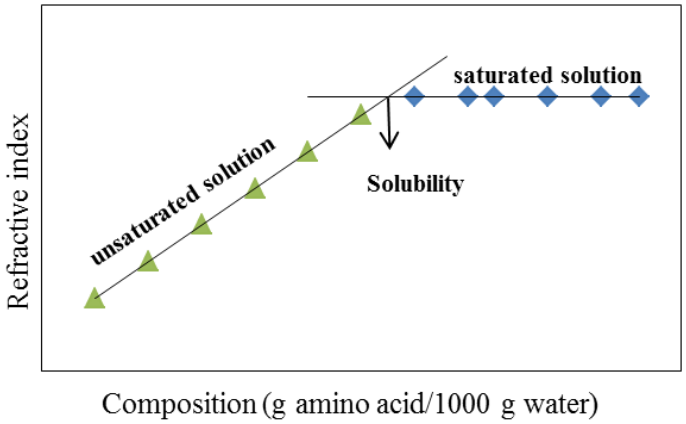

Figure 16 - Typical refractive index versus concentration of amino acid curve, obtained by applying method B.

- As previously, all the solutions were continuously stirred for 48 hours and, after this period, stirring was stopped. In the following 12 h, the solution was kept at rest.
- Samples were collected (1 cm^3) of the saturated liquid phase using plastic syringes and polypropylene filters (0.45 μm) previously heated to avoid precipitation of the amino acid.
- The method used for quantitative analysis relied on the refractive index measurement, using a refractometer (Abbemat 500, Anton Paar), shown in Figure 17, with a reproducibility of ±1 × 10^{-5}.

Figure 17 – Refractometer used in this work.

2.2. Results and discussion

2.2.1. Solubility in water

Data quality of amino acid/water binary systems can be checked by comparing the results obtained in this work with results already published in the literature. Table 4 shows that the solubility in pure water of the three amino acids considered in this work is in good agreement with the values obtained by other authors.

Table 4 - Comparison of the solubility of amino acids (g amino acid/1000 g of water) in pure water, at 298.15K.

Amino acid	Solubility(s)	$S_{average}$	$S_{this\ work}$
DL-alanine	165.8 Dunn *et al.* (1933) 165.44 Tomé *et al.* (2013) 169.3 Jin and Chao (1992) 167.2 Dalton and Schmidt (1933) 167.76 Kuramochi *et al.* (1996)	167.1	164.67
L-valine	58.449 Tomé *et al.* (2013) 58.399 Gekko (1981) 58.505 Gekko and Idota (1989) 58.458 Matsuo *et al.* (2002) 58.0 Sasahara and Uedaira (1993)	58.4	57.893
L-isoleucine	34.756 Tomé *et al.* (2013) 33.6 Ferreira *et al.* (2007) 34.9 Zumstein and Rousseau (1989) 32.0 Orella and Kirwan (1991) 32.4 Brown and Rousseau (1994) 32.3 Gekko *et al.* (1998) 34.1 Teja *et al.* (2002) 33.1 Matsuo *et al.* (2002) 33.3 Sasahara and Uedaira (1993)	33.4	33.472[a] 34.625[b]

[a]L-isoleucine supplied by Merck; [b]L-isoleucine supplied by Fluka.

2.2.2. Solubility in aqueous saline solutions

The solubilities of the amino acids in the aqueous solutions of the different salts, measured at 298.15 K, are presented in Tables 5-10, together with the correspondent standard deviation.

Table 5 - DL-alanine, L-valine and L-isoleucine solubility at 298.15 K in aqueous solutions of K_2SO_4, measured by the experimental method A.1.

	Salt molality	S (g/1000g de water)	Standard deviation
DL-alanine	0.00	164.67	0.05
	0.20	168.19	0.01
	0.40	167.55	0.14
	0.50	166.54	0.06
L-valine	0.00	57.893	0.031
	0.20	56.930	0.070
	0.40	53.950	0.093
	0.50	52.272	0.169
L-isoleucine	0.00	34.625	0.137
	0.20	33.727	0.049
	0.40	31.671	0.380
	0.50	30.327	0.163

Table 6 - L-valine and L-isoleucine solubility at 298.15 K in aqueous solutions of LiCl, measured by the experimental method A.2.

	Salt molality	S (g/1000g de water)	Standard deviation
L-valine	0.00	57.893	0.031
	1.00	59.279	0.045
	2.00	58.579	0.123
L-isoleucine	0.00	33.442	0.036
	1.00	34.365	0.088
	2.00	32.217	0.077

Table 7 - L-valine and L-isoleucine solubility at 298.15 K in aqueous solutions of Li_2SO_4, measured by the experimental method A.2.

	Salt molality	S (g/1000g de water)	Standard deviation
L-valine	0.00	57.893	0.031
	1.00	49.530	0.065
L-isoleucine	0.00	33.442	0.036
	1.00	23.043	0.045

Table 8 - DL-alanine, L-valine and L-isoleucine solubility at 298.15 K in aqueous solutions of $CaCl_2$, measured by the experimental method A.2.

	Salt molality	S (g/1000g de water)	Standard deviation
DL-alanine	0.00	164.67	0.05
	0.50	198.58	0.05
	1.00	232.75	0.10
	2.00	283.14	0.93

L-valine	0.00	57.893	0.031
	0.50	69.794	0.100
	1.00	74.381	0.078
L-isoleucine	0.00	33.442	0.036
	0.50	41.971	0.117
	1.00	43.215	0.807

Table 9 - L-valine and L-isoleucine solubility at 298.15 K in aqueous solutions of $Al_2(SO_4)_3$, measured by the experimental method B.

	Salt molality	S (g/1000g de water)	Standard deviation
L-valine	0.00	57.893	0.031
	0.50	140.820	0.618
L-isoleucine	0.00	33.442	0.036
	0.50	80.285	0.222

Table 10 - L-valine and L-isoleucine solubility at 298.15 K in aqueous solutions of $AlCl_3$, measured by the experimental method B.

	Salt molality	S (g/1000g de water)	Standard deviation
L-valine	0.00	57.893	0.031
	0.50	137.96	0.501
L-isoleucine	0.00	33.442	0.036
	0.50	95.457	0.633

Figure 18 shows the relative solubility of the three amino acids, in aqueous solutions of LiCl, $CaCl_2$, Li_2SO_4 and K_2SO_4.

(a)

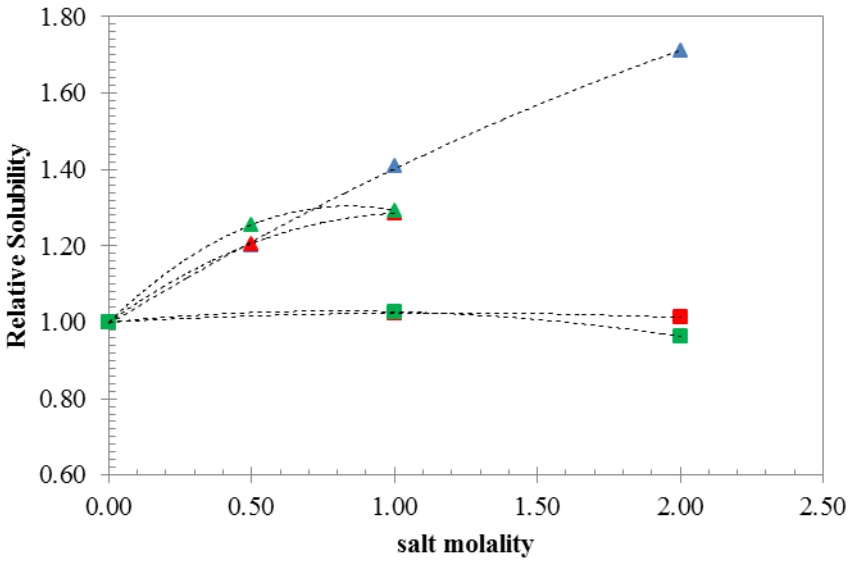

(b)

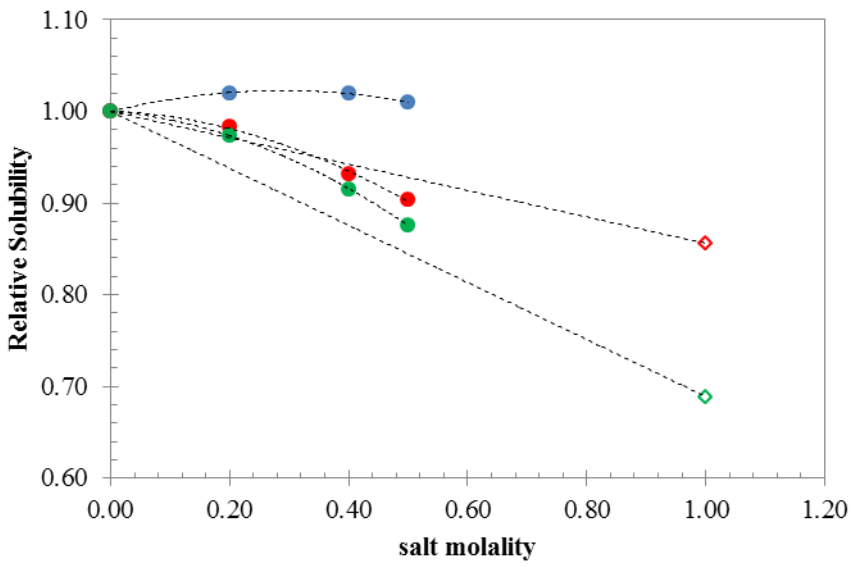

Figure 18 - Relative solubility of alanine (blue), valine (red), and isoleucine (green) in aqueous solutions, at 298.15 K, containing the salt: (a) □, LiCl; Δ, $CaCl_2$; and in (b) ◊, Li_2SO_4; ○, K_2SO_4. Lines are guides to the eyes.

As can be seen from Figure 18 (a), LiCl does not have a significant effect on the aqueous solubility of both amino acids. Nevertheless, at higher salt concentrations, the *salting-out* effect is more pronounced for Ile than in the case of Val. As shown in Figure 18 (b), Li_2SO_4 promotes the *salting-out* of Val and Ile. In this case, it was only possible to determine the solubility at 1 salt molality due to experimental difficulties. K_2SO_4, Figure 18 (b), also induces a similar *salting-out* effect for Val and Ile. In the case of Ala, a slight *salting-in* effect is observed, followed by a decrease in the solubility.

Figure 18 (a) also shows that $CaCl_2$ induces a pronounced *salting-in* of all the amino acids studied, being more significant for Ala. In the case of Val and Ile, a similar behavior is observed. This divalent cation seems to be a strong *salting-in* agent similar to Mg^{2+} (Tomé *et al.* 2013). No studies were performed using $CaSO_4$, due to its low solubility in water (Table 2).

To further study the cation specific effects on the amino acids aqueous solubility, a trivalent cation was used. The behavior of Al^{3+} is quite different from that observed in other systems, as both aluminum salts induce an exceptionally strong *salting-in* effect. In fact, a salt molality of 0.5 is sufficient to promote a large increase in the solubility of the amino acids, while, in other systems, a considerably higher salt molality is not enough to attain this effect.

The results obtained in this work were also compared with other data published in the literature, obtained by El-Dossoki (2010) for DL-alanine in aqueous solutions of K_2SO_4 and

$CaCl_2$, according to Table 1. As can be seen in Figure 19, a stronger *salting-in* was obtained by El-Dossoki (2010) for the aqueous solutions of K_2SO_4. As will be discussed later, in Chapter 3, our results are more consistent with the molecular dynamics simulations data gathered.

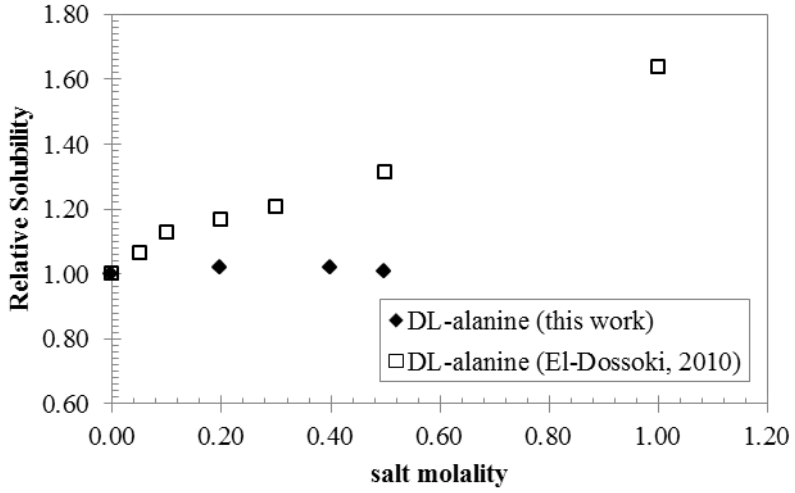

Figure 19 - Relative solubility of DL-alanine in potassium sulfate aqueous solutions obtained in this work and by El-Dossoki (2010), at 298.15 K.

Figure 20 shows a comparison of the relative solubility of the studied amino acid (Ala) in aqueous solutions containing $CaCl_2$ with results obtained by El-Dossoki (2010). In this case, a similar and significant *salting-in* effect is observed.

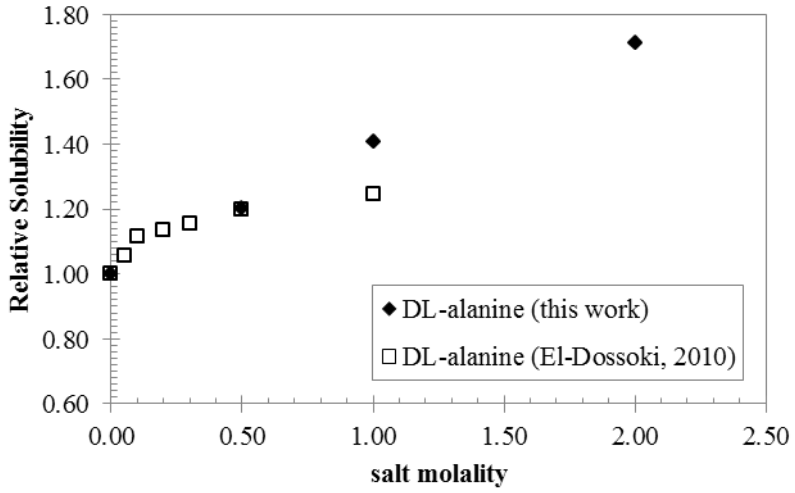

Figure 20 - Relative solubility of DL-alanine in $CaCl_2$ aqueous solutions obtained in this work and by El-Dossoki (2010), at 298.15 K.

2.2.3. pH measurements

In order to verify the pH effect on the amino acids solubility, pH measurements were also performed. At the end of the solubility experiments, the pH of the amino acid solutions was measured (pH meter inoLab pH 720, WTW) for selected amino acids solutions, including the ones with the highest salt molality. The measured pH values are provided in Table 11.

Table 11 - pH values measured for amino acids studied in aqueous saline solution at 298 K.

Salt	Amino acid	Salt molality	pH
$AlCl_3$	L-valine	0.50	2.70
	L-isoleucine	0.50	2.44
$Al_2(SO_4)_3$	L-valine	0.50	2.46
	L-isoleucine	0.50	2.24
$CaCl_2$	L-valine	0.50	5.81
		1.00	5.69
	L-Isoleucine	0.50	5.88
		1.00	5.75
LiCl	L-valine	2.00	5.93
	L-isoleucine	2.00	5.85
Li_2SO_4	L-valine	1.00	6.11
	L-isoleucine	1.00	5.92

Chapter 3. Molecular Dynamics Simulation

3.1. Introduction

One of the main tools for the study of biological systems is molecular dynamics simulations. The use of this computational method has allowed great advances in the study of the molecular mechanisms behind the effect of salts on amino acids aqueous solubility, as well as proved to be a valuable tool for the investigation of biochemical systems, including aqueous solutions and aqueous saline solutions of amino acids, peptides and proteins (Lund *et al.* 2008, Tomé *et al.* 2010, Tomé *et al.* 2013).

MD simulations compute the motion of interacting particles (molecules, atoms, ions, etc) in models of the three physical phases of matter. The key idea present here is to generate information at the microscopic level from the progression of the particles motion, by describing how the atomic positions, the velocities and the orientations change with time (Haile 1997). These simulations consist of the numerical solution of the classical equations of motion, for which the calculation of the forces acting on the particles is needed. These are, for their turn, obtained from a potential energy function (Allen 2004).

The potential energy $V(r_1, \dots, r_N)$ for a system at time t_i can be expressed in classical mechanics as the function of atomic positions using components such as bond-stretching, angle-bending, proper (and improper) dihedral angle rotations, having a part referring to the bonded interactions as well as a part representing the non-bonded interactions between the particles. As far as the latest are concerned, and for most simulations, it is usual to consider only a pair potential term, for which the Lennard-Jones form is the most commonly used. If electrostatic interactions are present, the Coulomb potentials must also be added. (Allen 2004, Fadda and Woods 2010).

The potential function used has thus the general form:

$$V(r_1, \dots, r_N) = \sum_{i<j} \frac{1}{2} k_{ij}^b (r_{ij} - r_{ij}^0)^2 + \sum_{i<j<k} \frac{1}{2} k_{ijk}^\theta (\theta_{ijk} - \theta_{ijk}^0)^2 + \sum_{i<j<k<h} \frac{1}{2} k_\varphi (1 + \cos(n\varphi + \gamma)) + \sum_{i<j} \frac{1}{4\pi\varepsilon_0} \frac{q_i q_j}{\varepsilon_r R_{ij}} + \sum_{i<j} 4\epsilon_{ij} \left[\left(\frac{\sigma_{ij}}{R_{ij}} \right)^{12} - \left(\frac{\sigma_{ij}}{R_{ij}} \right)^{6} \right] \quad (1)$$

Where k_{ij}^b is the bond-stretching constant, r_{ij}^0 is the equilibrium distance, k_{ijk}^θ is the angle-bending constant and θ_{ijk}^0 is the equilibrium angle. k_φ, n and γ are the torsion constant,

multiplicity and phase angle, respectively. q_i and q_j are point charges and R_{ij} is the distance between them, ε_r is the dielectric constant and ε_0 is the dielectric permittivity in *vacuo*. ϵ_{ij} and σ_{ij} are Lennard Jones repulsion-dispersion parameters, defined for each atom pair.

The first three terms refer to the potential energy associated with bond-stretching, angle-bending, and proper (and improper) dihedral angle rotations, respectively. The last two terms refer to the pairwise electrostatic interaction and to the repulsion-dispersion potential terms, respectively. The valence interactions, modeled in most biomolecular force fields by bond-stretching, angle-bending and dihedral terms, require the determination of force constants and equilibrium values for the distances and angles. The equilibrium values are not necessarily experimentally observed values. They can be calculated through quantum mechanics (Fadda and Woods 2010). Classical force fields are defined by the functional form of these components and by a set of parameters required by each term (Fadda and Woods 2010).

The choice of the force field is one of the most important aspects when performing MD simulations, having a significant repercussion on the accuracy of the results (Hess *et al.* 2008, Yoo and Aksimentiev 2011). Among others (Chandrasekhar *et al.* 1984, Smith and Dang 1994, MacKerell *et al.* 1998, Weerasinghe and Smith 2003), the Optimized Potentials for Liquid Simulations (OPLS) has been one of the most frequently used. In this work, the OPLS force field was employed because it has proved to provide accurate descriptions of aqueous saline solutions of amino acids and it has been shown that, although the degrees of binding are affected by the model chosen, the relative changes along the Hofmeister series are unchanged (Tomé *et al.* 2012, Tomé *et al.* 2013).

To perform molecular dynamics simulation calculations some fundamentals steps are required. First, initial positions are ascribed to a set of *N* particles that are going to fill a MD box. The initial velocity of each particle introduced in the MD box is established. Then, the intermolecular potential energy is calculated and the forces acting on each of the *N* molecules of the MD box are derived. Next, the Newton´s equations are integrated for each particle, using numerical algorithms. After these steps, the system is let to progress in time during, first, n_e and then n_p steps, where n_e is the necessary number to achieve the equilibrium (order of 10^3) and n_p is the necessary number to achieve a good statistics (order of 10^3-10^4). Ultimately, the time averages over the number of steps n_p are calculated (Fernandes 1988, Allen 2004).

The theoretical foundations of MD are based on the contributions of well-known names of analytical mechanics. In its most simple form, for structureless particles, molecular dynamics simulations involve little more than Newton' second law. For rigid molecules, it is necessary to use Euler equations and, in the case of molecules with internal degrees of freedom and subject to structural constraints, the Lagrange's method might be applied (Rapaport 2004). With the theoretical, numerical and computational development witnessed in the past decades, new algorithms have been developed and MD simulation methods have become more and more powerful and effective (Allen 2004).

Molecular dynamics simulations serve as a complement for the conventional experiments, allowing to learn something new or something that cannot be found in other ways. These computational methods work like a bridge between length and microscopic time scales and the macroscopic world of the laboratory, providing insights into the molecular interactions established in the systems and accurate predictions of their properties. Through MD simulations, it is possible to reveal details that are hidden in the experience as well as to calculate properties that are harder or impossible to obtain in the laboratory, e.g. conditions of extreme temperature or pressure (Allen 2004).

3.2. Computational method

To investigate the interactions between salts and amino acids, the procedure recently applied by Tomé et al. (2013) was adopted.

In the MD simulations, amino acids in the zwitterionic form (pH=7) were modelled in aqueous saline solutions, using the GROMACS 4.04 molecular dynamics package (Hess *et al.* 2008) and the isothermal-isobaric N*pT* ensemble (T=298.15 K and p=1 bar). The Nosé-Hoover thermostat and the Parrinello-Rahman barostat were used (Parrinello and Rahman 1981, Nosé 1984) to fix the temperature and pressure, respectively. The equations of motion were integrated with the Verlet-Leapfrog algorithm, with a time step of 2 fs (Hockney *et al.* 1974).

To study the selected systems, amino acids, ions and water molecules were randomly placed in a simulation cubic box that was generated with lateral dimensions of 45 Å. Periodic boundary conditions were applied in three dimensions.

For all MD simulations, an amino acid concentration of 0.35 mol dm^{-3} and a salt concentration of 1.0 mol dm^{-3} were reproduced, except in the case of the salt K_2SO_4 for which

(due to its lower aqueous solubility) a concentration of 0.50 mol dm^{-3} was considered. Therefore, in the case of a salt concentration of 1.0 mol dm^{-3}, 6 amino acid molecules, 900 water molecules and 17 cation-anion pairs were included in each box whereas, for the case of salt concentration of 0.5 mol dm^{-3}, 6 amino acids molecules, 900 water molecules and 9 cation-anion pairs were incorporated.

To begin, a 10 000 step energy minimization of the system was performed, followed by two simulations, one for equilibration and the final for production. For the equilibration simulation the number of steps was 50 000 and for the production simulation 10 000 000. After equilibration, the volume of the box ranged from 27.8 to 29.9 nm^3, depending on the system.

To describe the dispersion/repulsion forces between pairs of neighboring atoms, the Lennard-Jones potential was used and the electrostatic interactions were described using the point-charge Coulomb potential. Long-range electrostatic interactions were accounted for using the particle-mesh Ewald method (Essmann *et al.* 1995) with a cutoff of 1.0 nm for the real-space part of the interactions. A cutoff radius of 1.2 nm was used for the Lennard-Jones potential. The bond lengths were held rigid using the LINCS constrain algorithm, angle bending was modelled by an harmonic potential and dihedral torsion by a Ryckaet-Bellemans function (Hess *et al.* 1997).

According to literature, the force fields selected for this work have provided accurate descriptions of aqueous saline solutions of amino acids (Aaqvist 1990, Tomé *et al.* 2010, Tomé *et al.* 2013). In the case of water, SPC/E model was used, while for the amino acids and for the chloride, lithium, calcium and potassium ions the OPLS-all atom force field was applied (Berendsen *et al.* 1987, Aaqvist 1990). For the sulfate anions, the second (std2) force field model proposed by Cannon et al. (Cannon *et al.* 1994) was used, and for the aluminum cations the force field parameters were taken from the work of Faro et al. (Faro *et al.* 2010).

3.3. Results and discussion

Aiming to understanding, at a molecular level, the specific effects of ions on the aqueous solubility of the amino acids experimentally observed, MD simulations were performed. The structure and atom labeling of the amino acids studied are displayed in Figure 21.

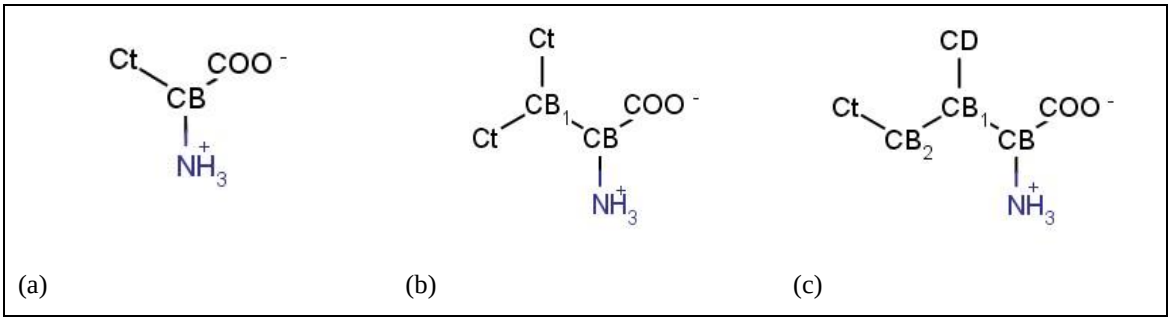

Figure 21 - Structure and atom labeling of the amino acids studied in this work: (a) alanine (Ala), (b) valine (Val) and (c) isoleucine (Ile). C_t stands for the terminal carbon atom of the amino acid side chain and C_B is used to denote the carbon backbone of the amino acid side chain.

The radial distribution functions (RDF) can be used to describe the structural organization of a system. This function gives the possibility of finding a particle at a distance *r* from another particle (considering a reference particle). RDFs are very useful to help interpreting experimental results (Batista *et al.* 2012), providing a description of enhancement (values larger than 1) or depletion (values smaller than 1) of densities of atoms or groups of atoms around a selected moiety, with respect to bulk values (Batista *et al.* 2012, Tomé *et al.* 2013).

Throughout this work, RDFs were calculated and analyzed for all possible interactions that involve the constituting groups of the amino acids, the cations, the anions and water. However, only the most relevant RDFs, corresponding to the interactions at the level of the atoms representative of the non-polar part and of the charged moieties of the amino acids (amine and carboxylic group), will be presented.

Along this chapter, it will become clear that the behavior of the studied amino acids is somehow similar. Thus, the RDFs of the amino acid Isoleucine (Ile) will be presented here, while those of Alanine (Ala) and Valine (Val) will be presented in Appendix A. To help in the analysis of the RDFs, values for the position and intensities of the RDF peak maxima corresponding to the interactions of selected groups of Ile in the aqueous saline solutions are also provided in the Appendix (Table A.1).

Although the MD results have been obtained at pH=7 (zwitterionic form), throughout the discussion that follows the experimental data will be used to support the simulation data, since at the pH of the experimental measurements (Table 11) the zwitterionic form is still present even for the systems containing aluminum (Nelson and Cox 2008). Furthermore, the MD calculations for K_2SO_4 systems were performed for a different concentration of the salt. Although the

concentration parameter is introduced and the intensity of the RDF peaks is likely to be affected, this is not, as will be seen, relevant for the global interaction patterns discussed.

3.3.1. Anion effect

In Figures 22-25, the radial distributions functions corresponding to the interactions of the C_t and C_B atoms (representative of the non-polar moieties) and of the hydrogen atom of the amino and the oxygen atom of the carboxyl group (representative of the charged part) of Ile with the anions of all the studied salts are presented.

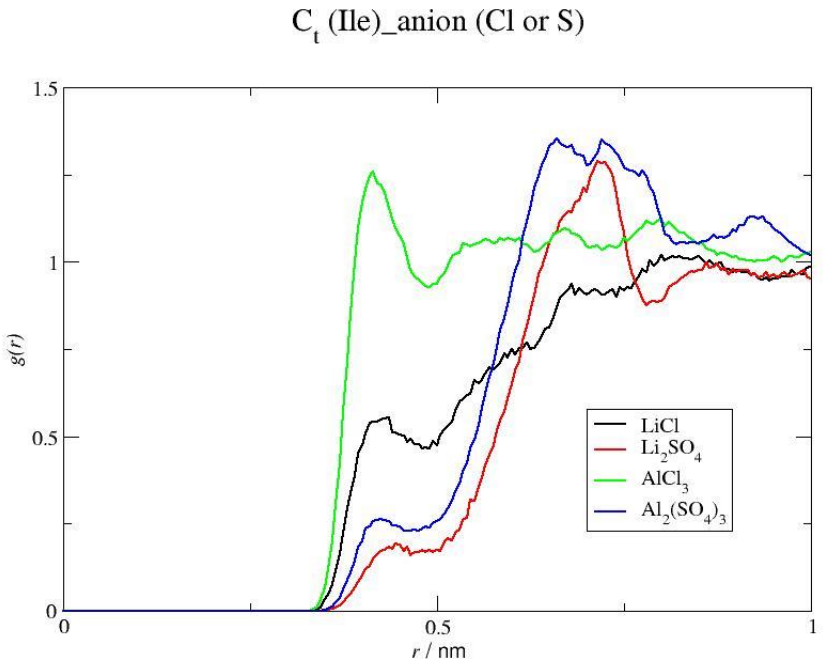

Figure 22 - Radial distribution functions corresponding to the interactions of isoleucine C_t with the central atom of the anions (Cl or S), for salts containing Li^+ and Al^{3+} cations.

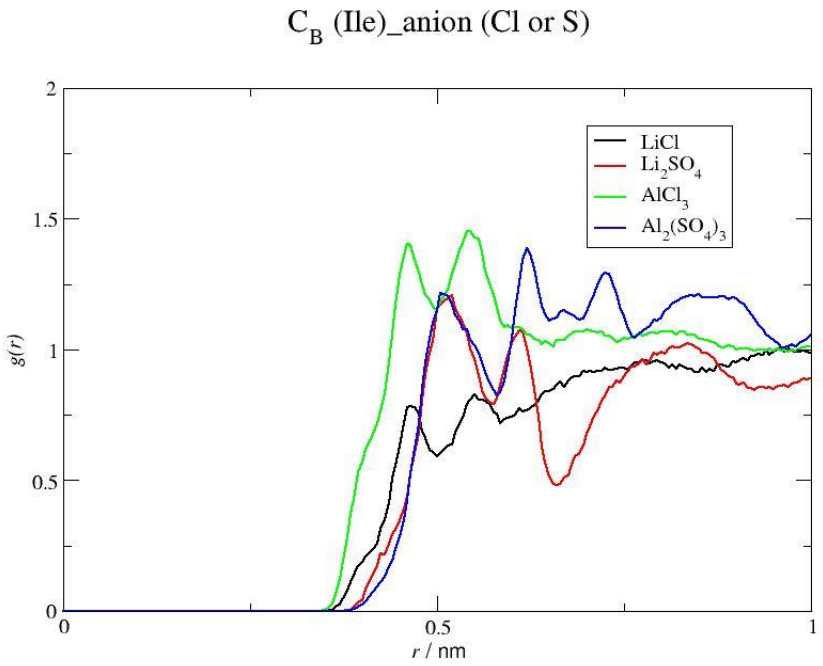

Figure 23 - Radial distribution functions corresponding to the interactions of isoleucine C_B with the central atom of the anions (Cl or S), for salts containing Li^+ and Al^{3+} cations.

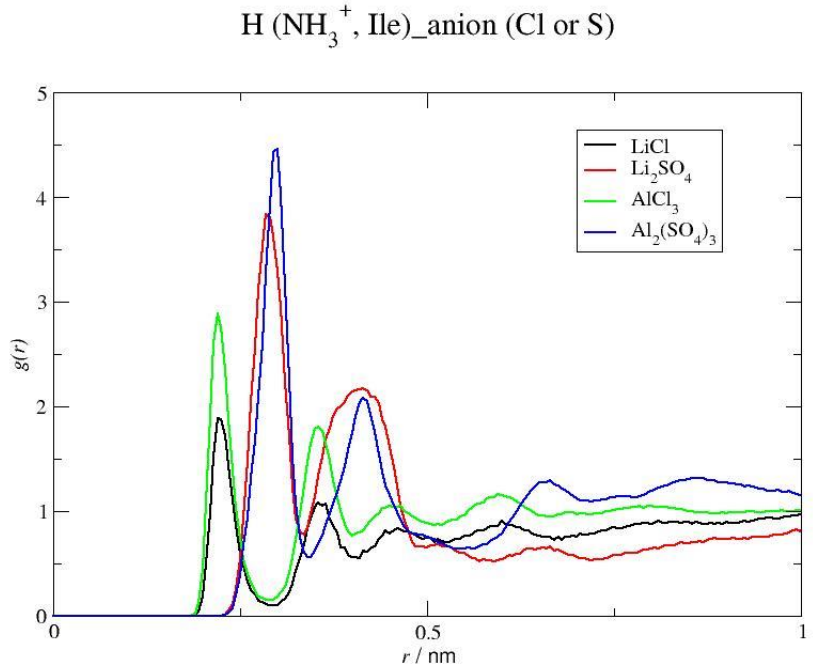

Figure 24 - Radial distribution functions corresponding to the interactions of the H atom of the amine group of isoleucine with the central atom of the anions (Cl or S), for salts containing Li^+ and Al^{3+} cations.

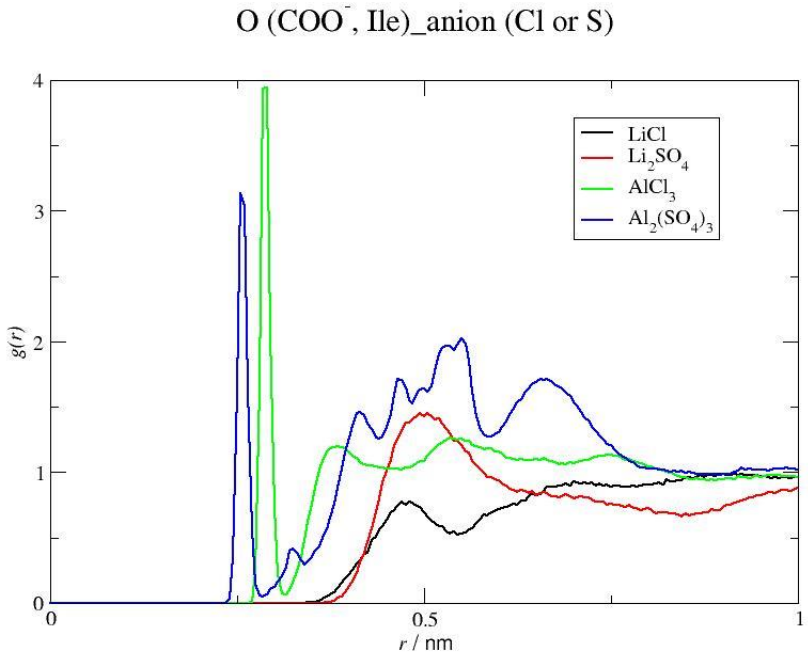

Figure 25 - Radial distribution functions corresponding to the interactions of the O atom of the carboxylic group of isoleucine with the central atom of the anions (Cl or S), for salts containing Li^+ and Al^{3+} cations.

As can be seen in Figure 22 and Figure 23, the interaction of the anions (Cl^- and SO_4^{2-}) with C_t and C_B of Ile is quite weak, as indicated by the RDFs peaks which present values slightly higher than 1 and appear at large distances (Table A.1). Although the distribution of both anions does not reveal their presence in the first solvation layer around the non-polar moieties of the amino acid, slightly more pronounced interactions are observed in the case of $AlCl_3$, and the RDF peaks of the sulfate salts appear at larger distances when compared to the chlorides.

The RDFs referring to the interactions of the H and O atoms of the amine and the carboxylic groups of Ile with the anions are represented in Figure 24 and Figure 25 respectively, and show a clear association of Cl^- and SO_4^{2-} to the charged groups.

In Figure 24, it is possible to observe that the peaks corresponding to the interactions of the SO_4^{2-} ions with the positively charged group of Ile are the most intense; however, the peaks referring to the interactions of Cl^- appear at shorter distances. This result might be due to the sulfate being a divalent anion and to the smaller size of Cl^- which enables this ion to get closer to the amine group.

As suggested by the results of Figure 25, significant interactions are observed between the negatively charged group of Ile and the anions of $Al_2(SO_4)_3$ or $AlCl_3$, while almost no affinity for COO^- is exhibited by the lithium salts, as expected due to the electrostatic repulsion. This is a consequence of the presence of the Al^{3+} cations which shield unfavorable interactions between SO_4^{2-} anions and the COO^- group, promoting an indirect binding.

Relatively to the other amino acids studied (Ala and Val), they present a similar behavior to Ile, as can be observed in Figures A.1-A.3 and Figures A.4-A.6, respectively. However, the interactions are globally stronger in the case of Ala, probably due to the smaller size of this amino acid.

These results are in agreement with those previously reported and support the mechanism proposed by Tomé et al. (Tomé *et al.* 2010) for the effect of the anions on the amino acids aqueous solubility. In fact, the analysis of the MD results obtained in the current work suggests that SO_4^{-2} does not establish important interactions with the non-polar moieties of the amino acids and interacts with the positively charged group, having a tipical behavior of a *salting-out* inducing anion.The interaction of the high charge density SO_4^{2-} anion with a hydrophobic moiety of the amino acid is a highly unfavorable process; thus, this anion excludes itself from the vicinity of the non-polar groups of the amino acid due to its preferencial hydration. As a result, the solubility of the amino acid in water decreases. The Cl^- anion does not either establish important interactions with the non-polar part of the amino acids, only with the amino group, and will thus have a negligible effect on the solubility, or at least a slight *salting-out* since it avoids the non-polar moieties. Further evidence for these interpretations can be obtained from: (i) the values of the thermodynamic properties of hydration displayed in Table 12 which show a highly favourable hydration of the sulfate anion; (ii) from the RDFs presented in Figures 22-26 which suggest a stronger interaction of the sulfate anion with water than with the amino acids, and (iii) from the values calculated for the energies of selected interactions of Ile systems provided in Table 12, which show globally less favourable Lennard-Jones terms for the energies of the (amino acid-anion) interactions in the case of SO_4^{2-} systems and (amino acid-water) interactions generally more favorable than (amino acid-anion), when comparing to the correspondent chloride salt comprising the same cation.

Table 12 - Values ($kJmol^{-1}$) of the Lennard-Jones (LJ) and Coulomb (Coul) terms of the energies calculated for the interactions (amino acid-water), (amino acid-anion) and (amino acid-cation) for the different systems under study.

Salts	Interactions	LJ	Coul
LiCl	aa-water	45,4	-2484,4
	aa-anion	-2,5	-43,1
	aa-cation	-4,6	-26,3
Li_2SO_4	aa-water	22,6	-2204,2
	aa-anion	-2,8	-244,6
	aa-cation	-9,5	-42,8
$CaCl_2$	aa-water	-48,9	-1215,0
	aa-anion	-3,0	-102,3
	aa-cation	134,7	-1733,1
K_2SO_4	aa-water	16,8	-2273,0
	aa-anion	1,1	-208,8
	aa-cation	4,7	-52,5
$AlCl_3$	aa-water	26,6	-336,9
	aa-anion	18,4	-92,4
	aa-cation	358,4	-5525,7
$Al_2(SO_4)_3$	aa-water	109,5	-1030,4
	aa-anion	65,3	-28,5
	aa-cation	187,4	-3549,5
Water	aa-water	33,8	-2560,6

These results are in agreement with the strong *salting-out* effect experimentally observed in aqueous solutions of sulfate salts (Arakawa and Timasheff 1984, Tomé *et al.* 2013), a strongly hydrated anion positioned in the extreme of the Hofmeister series, and with the less pronounced effects of chloride salts (Tomé *et al.* 2010), an anion positioned in the middle of the series. They are also consistent with the experimental results obtained in this work for the *salting-out* effects of the LiCl, Li_2SO_4 and K_2SO_4 salts. Differences in the magnitude or direction of the solubility effects promoted are related to the influence of other factors which will be discussed in the following sections.

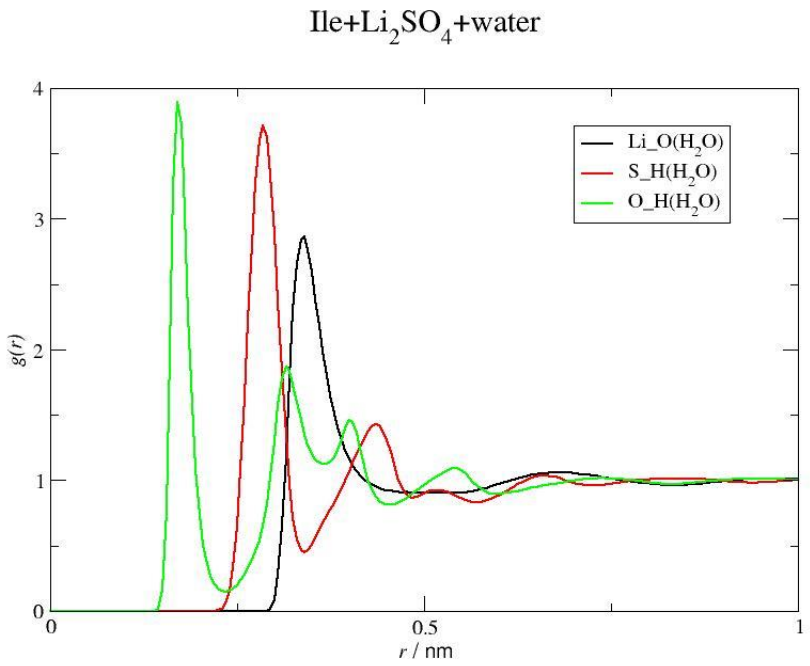

Figure 26 - Radial distribution functions corresponding to the interactions of Li_2SO_4 salts with water molecules, in the presence of isoleucine.

3.3.2. Cation effect

In this section, the more relevant interactions between selected atoms of the amino acids and the cations of all the studied salts are discussed.

In Figures 27-30, the RDFs corresponding to the interactions of the cations (Li^+,K^+,Ca^{2+} or Al^{3+}) with the carbon atoms representative of the non-polar moieties and with the negatively charged group of Ile are presented. The RDFs of Ala and Val are provided in Figures A.3 and A.4 of the Appendix.

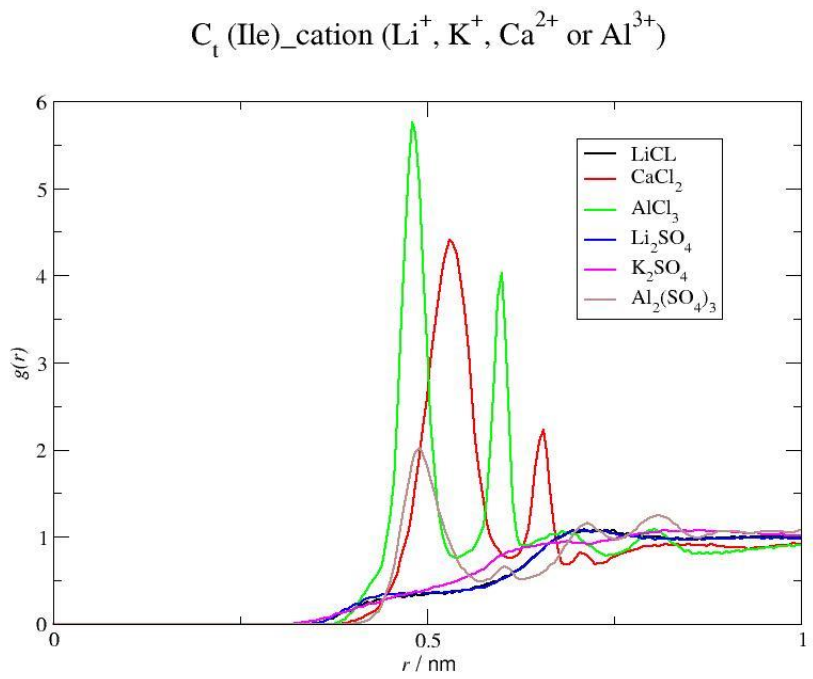

Figure 27 - Radial distribution functions corresponding to the interactions of isoleucine C_t with the cations (Li^+, K^+, Ca^{2+} or Al^{3+}) for all the studied salts.

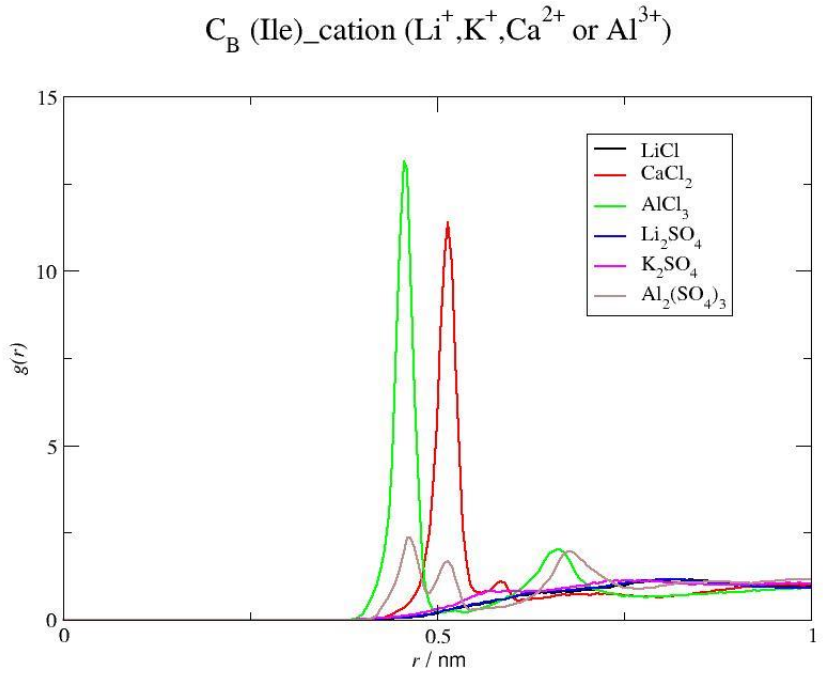

Figure 28 - Radial distribution functions corresponding to the interactions of isoleucine C_B with the cations (Li^+, K^+, Ca^{2+} or Al^{3+}) for all the studied salts.

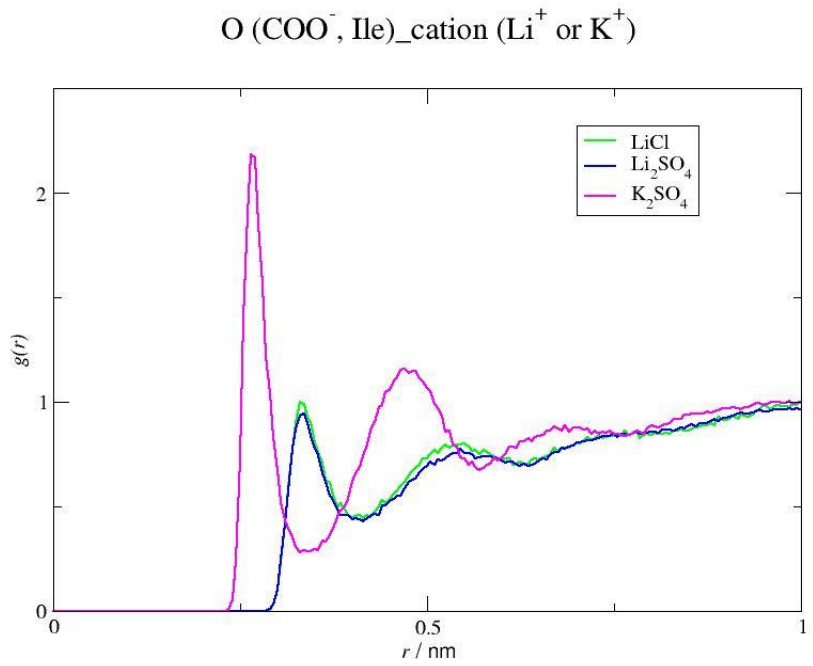

Figure 29 - Radial distribution functions corresponding to the interactions of the O atom of the carboxylic group of isoleucine with the monovalent cations (Li^+ or K^+) for all the studied salts.

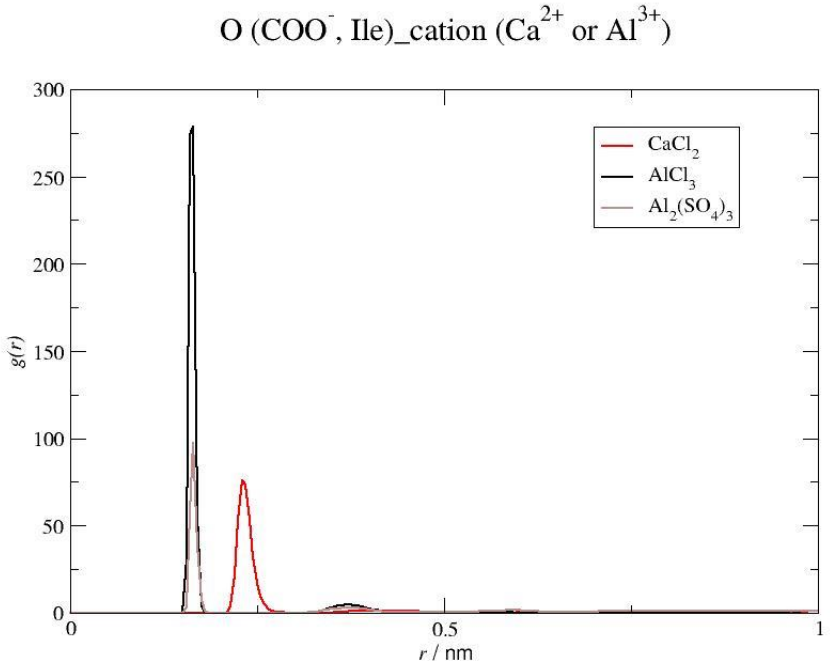

Figure 30 - Radial distribution functions corresponding to the interactions of the O atom of the carboxylic group of isoleucine with the polyvalent cations (Ca^{2+} or Al^{3+}) for all the studied salts.

In Figure 27 and Figure 28, it is possible to observe the RDFs corresponding to the interactions of the studied cations with the non-polar moieties (C_t and C_B) of Ile. As suggested by the intensity and position of the peaks, these interactions are absent in the case of the salts of the monovalent lithium and potassium ions and occur only in a second solvation layer for the systems comprising the polyvalent Al^{3+} and Ca^{2+}. The strongest RDF peaks referring to (C_t/C_B-cation) interactions are observed for $AlCl_3$ aqueous solutions and the weakest for $Al_2(SO_4)_3$. Both occur, though, at shorter distances than in the case of $CaCl_2$. The RDF peaks corresponding to the interactions of the cations with C_B of Ile are more intense relatively to the terminal carbon C_t, probably because C_B is closer to the charged COO^-group.

The interactions of the polyvalent cations with the negatively charged group of Ile are extremely strong, being significantly stronger in the case of salts containing Al^{3+}. Indeed, as can be observed in Figure 30 and Table A.1, the peaks referring to the interactions of the cations Al^{3+} and Ca^{2+} with the O(COO^-) atoms are extraordinarily intense and occur at very short distances. Their strength decreases in the order $AlCl_3 > Al_2(SO_4)_3 > CaCl_2$, as shown by the values of (r/nm, g(r)) of the peak maxima displayed in Table A.1, which are (0.166; 217.101), (0.165; 97.094) and (0.231; 75.574), respectively. For the monovalents cations, the interactions (O(COO-)$^-$cation) are by far significantly weaker. In the case of the salts containing K^+, there is yet some association while in the case of the salts containing Li^+, the interaction is pratically nonexistent. As can be observed in Figure 29 and Table A.1, the peak corresponding to the interaction of the cation of the salt K_2SO_4 presents an intensity above 2, while in the case of the RDF peak corresponding to the interaction of the cation of the salts LiCl or Li_2SO_4, the intensity is very close to 1. This molecular picture can be vizualized from the snapshots obtained from simulations of aqueous solutions of Ile in the presence of the lithium and aluminum salts presented in Figures 31-34, showing the relative positions of the ions around the carboxyl group and much shorter distances in the case of Al^{3+} than in the case of Li^+.

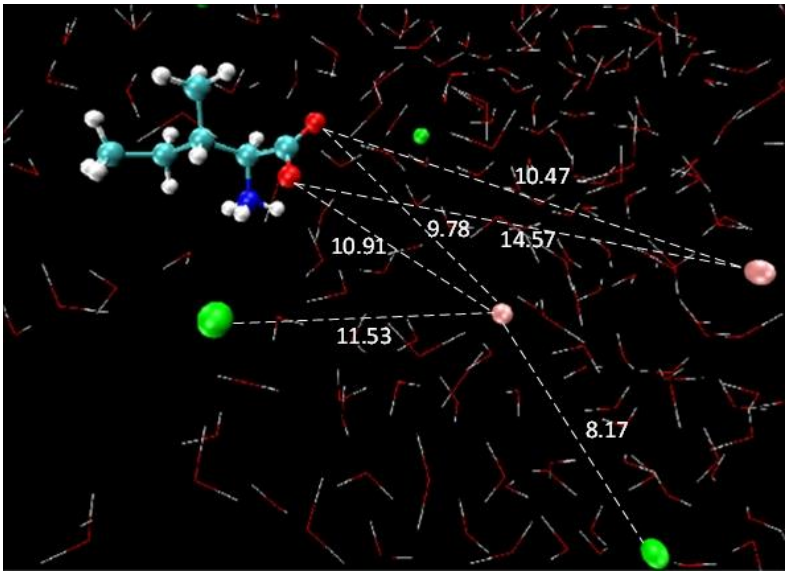

Figure 31 – Snapshot from a simulation of (Ile + LiCl + water) mixtures, showing the distances (Å) between selected atoms. Light blue spheres represent carbon atoms, dark blue spheres are nitrogen atoms, red spheres are oxygen, white spheres are hydrogen, green spheres are chloride and pink spheres are lithium. Water molecules are represented in line style.

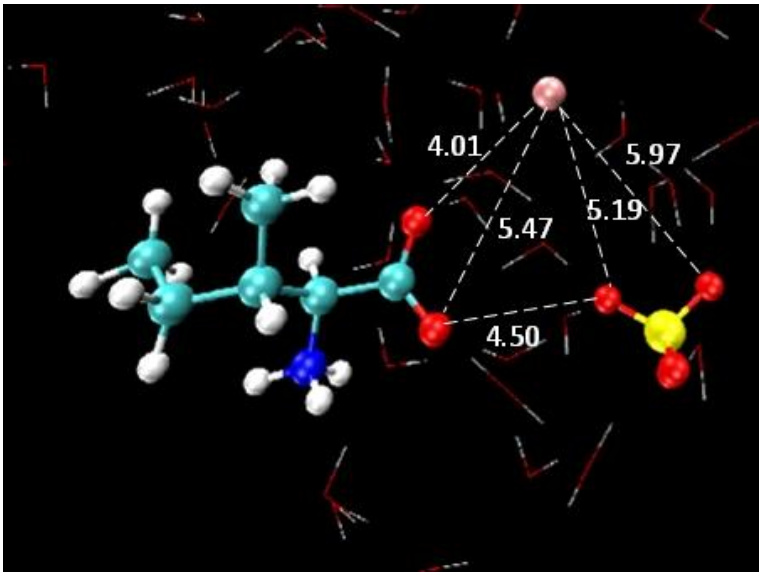

Figure 32 - Snapshot from a simulation of (Ile + Li_2SO_4 + water) mixtures, showing the distances (Å) between selected atoms. Light blue spheres represent carbon atoms, dark blue spheres are nitrogen atoms, red spheres are oxygen, white spheres are hydrogen, yellow spheres are sulfur and pink spheres are lithium. Water molecules are represented in line style.

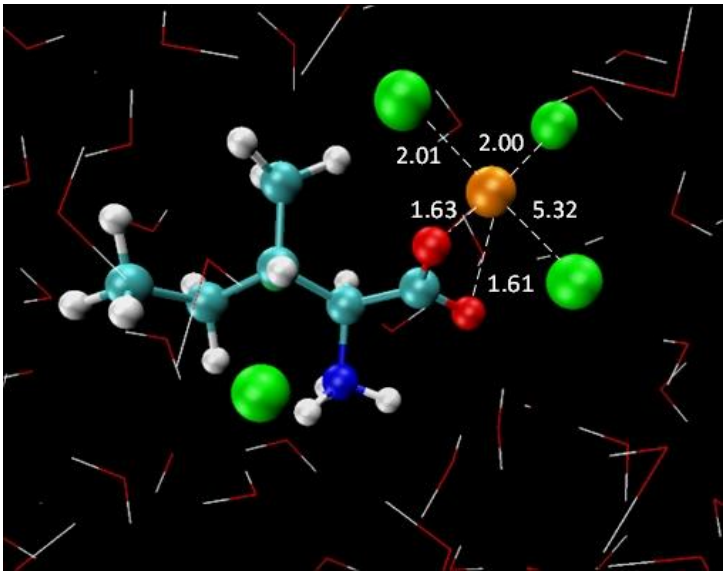

Figure 33 - Snapshot from a simulation of (Ile + $AlCl_3$ + water) mixtures, showing the distances (Å) between selected atoms. Light blue spheres represent carbon atoms, dark blue spheres are nitrogen atoms, red spheres are oxygen, white spheres are hydrogen, green spheres are chloride and orange spheres are aluminum. Water molecules are represented in line style.

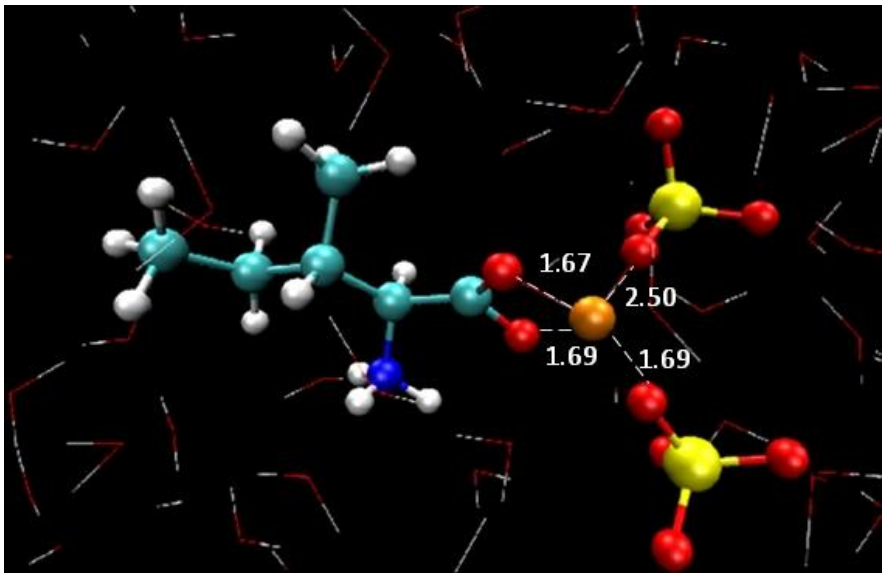

Figure 34 - Snapshot from a simulation of (Ile + $Al_2(SO_4)_3$ + water) mixtures, showing the distances (Å) between selected atoms. Light blue spheres represent carbon atoms, dark blue spheres are nitrogen atoms, red spheres are oxygen, white spheres are hydrogen, yellow spheres are sulfur and orange spheres are aluminum. Water molecules are represented in line style.

Relatively to Ala and Val, a similar behavior can be observed in Figures A.7-A.9 and Figures A.10-A.13, respectively. However, analyzing the peaks' intensity, there are differences due to the alkyl size chain that will be discussed later.

In Table 13, the molar entropy of hydration and the Gibbs free energy of hydration for all the studied ions is presented.

Table 13 - Molar entropy of hydration, $\Delta_{hyd}S$, and Gibbs free energy of hydration, $\Delta_{hyd}G$, at 298.15 K (Marcus, 1997).

Ion	$\Delta_{hyd}S$ ($J.K^{-1}.mol^{-1}$)	$\Delta_{hyd}G$ ($kJ.mol^{-1}$)	$\Delta_{hyd}H$ ($kJ.mol^{-1}$)
Cl^-	-75	-347	-367
SO_4^{2-}	-200	-1090	-1035
Li^+	-142	-481	-531
Ca^{2+}	-252	-1515	-1602
K^+	-74	-304	-334
Al^{3+}	-538	-4531	-4715

As can be seen, the calcium and aluminum cations present large energies of hydration and should, therefore, form hydration complexes that would contribute to a dehydration of the amino acids and their *salting-out*. However, that not is experimentally observed in this work; instead, Ca^{2+} and Al^{3+} behave as strong *salting-in* agents.

According to literature, some divalent cations are able to form charged and very soluble complexes with amino acids. Calcium ions can form such complexes with amino acids in aqueous solutions (Tian *et al.* 2002, Tomé *et al.* 2013). The analysis of the behavior of Ca^{2+} observed in Figure 30, suggests that this cation is able to form a complex with isoleucine, justifying the pronounced *salting-in* effect induced by $CaCl_2$. The same is verified for the other amino acids under study. Since the Al^{3+} cation presents a similar behavior, although with much more intense RDF peaks, it is possible to infer that this cation will also be able to form a complex with the studied amino acids, although no information on this subject is available in the literature.

In short, strongly hydrated polyvalent cations present extremely strong interactions with the carboxylic group of the amino acids and their binding to the non-polar moieties of the amino acids occurs only in a second solvation layer. The weakly hydrated monovalent cations establish almost non significant interactions with the carboxilic group of the amino acids and do not interact with their non-polar moieties. Therefore, it is expected that Li^+ and K^+ ions will have a small effect in the amino acid solubility (with Li^+ even smaller than K^+), being the effect induced by the salt governed by the nature of the anion. On the other hand, Ca^{2+} and Al^{3+}salts should have

a strong *salting-in* effect, in which the cation, or the cation and the anion, will govern the magnitude of the effect. These issues will be addressed in detail in the following paragraphs.

The simulation results obtained in this work are consistent with the molecular mechanism proposed by Tomé *et al*. (2013) for the effect of the cations on the aqueous solubility of amino acids. According to that molecular model, the mechanisms by which cations operate are more complex and distinct from that of the anions. *Salting-in* inducing (polyvalent) cations do not establish important (direct) interactions with the hydrophobic parts of the amino acids, but, due to their high charge density, are able to form charged complexes with the amino acids, which are very soluble, promoting therefore pronounced increases in their aqueous solubilities. This behavior was observed for the Mg^{2+} ion (Tomé *et al.* 2013) and it is also experimentally found in this work for the Al^{3+} and Ca^{2+} cations. Moreover, this reversal in the Hofmeister series for cations has been reported for systems of biomolecules containing sites with negative charges (Füser and Steinbüchel 2005, Kherb *et al.* 2012, Xie and Gao 2013). The differences found in the magnitude of the solubility effects induced by the salts comprising the polyvalent cations will depend on the nature of the cation and on the properties of the anion, as discussed below. On the other hand, weakly hydrated (monovalent) cations are not able to form those complexes probably because their interaction with water is more favorable than with the COO^- group. Their solubility influence will be thus much less significant and will be ruled by the molecular mechanism by which the *salting-out* anions operate. This behavior was observed for K^+ and Na^+ (Tomé *et al.* 2013) and comparatively less pronounced solubility effects were observed in this work for the potassium and lithium salts. The direction and magnitude of the effects induced by the salts of these monovalent cations will be dictated by the nature of the anion, as discussed below. The interaction energies (Table 12) support these results: for the polyvalent cations, the Coulomb terms of the energies corresponding to the (aa-cation) interactions are more favorable (less positive) than the (aa-water) ones and, for the monovalent cations, the opposite occurs. Furthermore, and as an example, the comparison of the RDF peaks of Figure 35, suggests that Al^{3+} interacts less with water than with the amino acid.

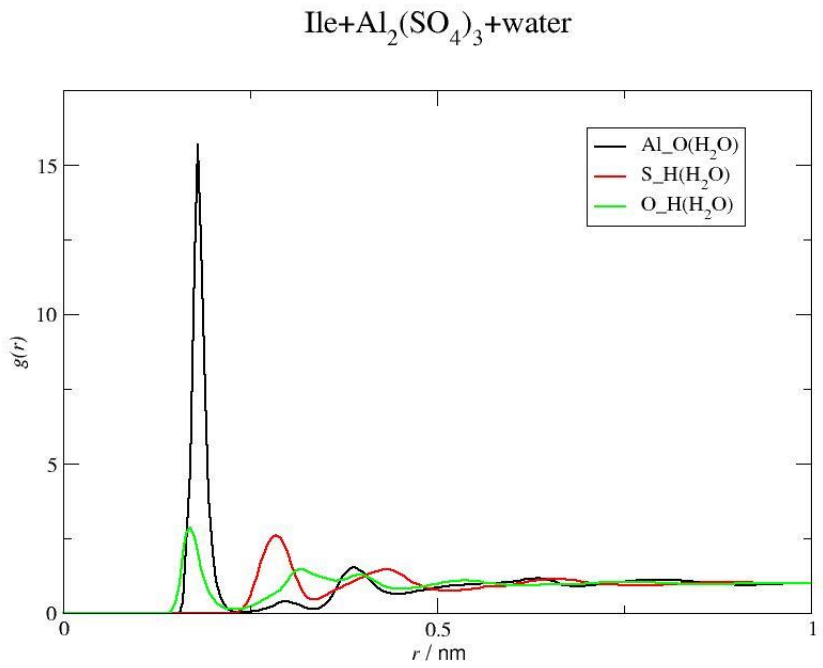

Figure 35 - Radial distribution function for the interactions between water molecules and the ions in aqueous solutions of Ile in the presence of $Al_2(SO_4)_3$.

As stated above, polyvalent cations will determine the direction of the solubility effect promoted by the salts, while the monovalent will have a less significant influence. In both cases, however, the magnitude or the magnitude/direction (respectively) will be determined by the properties of their counterion. To discuss this aspect, we will compare the results obtained for some groups of systems.

First, comparing the experimental results obtained for salts with strongly hydrated cations and weakly hydrated anions, it is possible to observe in Table 8, 9 Table 10 that, in general, the magnitude of the *salting-in* decreases in the order $AlCl_3$ > $CaCl_2$ ~ $MgCl_2$ (Tomé *et al.* 2013), consistently with the decrease observed in the RDF peaks referring to the (cation-O(COO-)) interactions (Figure 30) and with the data from Tomé *et al.* (2013). The intensity of these interactions is determined by the properties of the cation and dictates the magnitude of the solubility effect. On the other hand, when the salts comprise a strongly hydrated cation and also a strongly hydrated anion positioned in the extreme of the Hofmeister series, such as SO_4^{2-}, the presence of the latest leads to a decrease of the magnitude of the *salting-in* promoted by the cation. Nevertheless, this was only observed experimentally for L-isoleucine (Tables 9 and 10).

In agreement with the mechanism proposed by Tomé et al, there will be a competition between the interactions established by the cation and the anion and its balance will determine the magnitude of the solubility effect.

Finally, a comparison between the experimental and simulation results obtained for salts with weakly hydrated cations, such as LiCl and Li_2SO_4, is made (Tables 6 and 7). From the experimental results, a slight *salting-out* effect is observed in the presence of LiCl for Ile and for Val. However, in the case of Ile the *salting-out* effect is more pronounced, probably due to the effect of the amino acid non-polar chain. In the case of Li_2SO_4, the *salting-out* effect is stronger for both amino acids, being more pronounced in the case of Ile. Once again, this is, probably, due to the effect of the amino acid non-polar chain.

In fact, and as shown by the simulation results of this work, the salt LiCl, composed by weakly hydrated ions which do not significantly interact with the amino acids, has a small influence on the amino acids solubilities. But when the counterion is sulfate, a strong *salting-out* agent, the anion dominates the mechanism and controls the solubility effect since almost no interactions are established by the cation with the amino acids.

3.3.3. Interactions with water

In addition to the previous calculations, RDFs were also calculated for all the possible interactions involving the amino acids and water molecules. In Figures 36-38, the RDF peaks corresponding to the interaction of the different molecular regions of isoleucine with water molecules are shown, in the presence of all the studied salts, as well as in their absence.

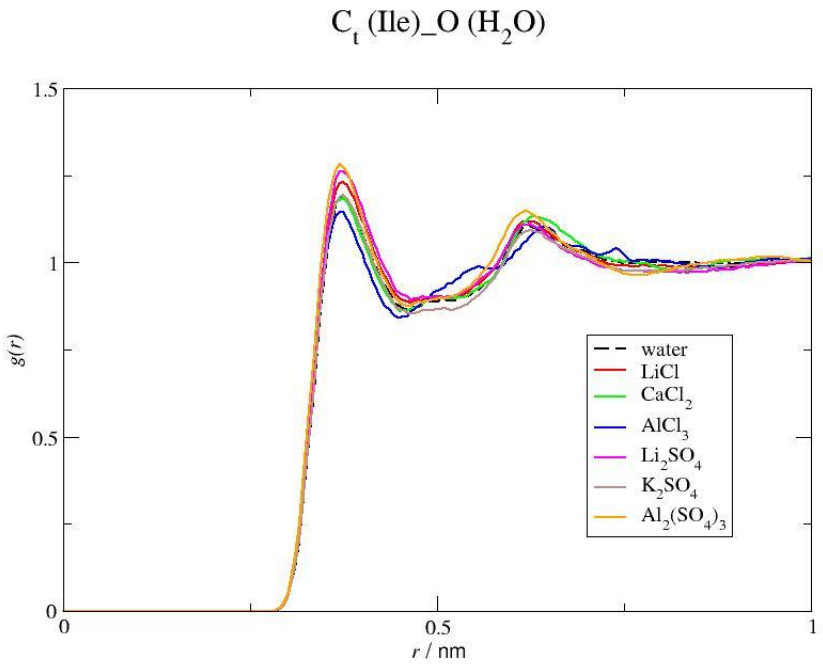

Figure 36 - Radial distribution functions corresponding to the interaction of isoleucine C_t with water molecules, in the presence of all the studied salts.

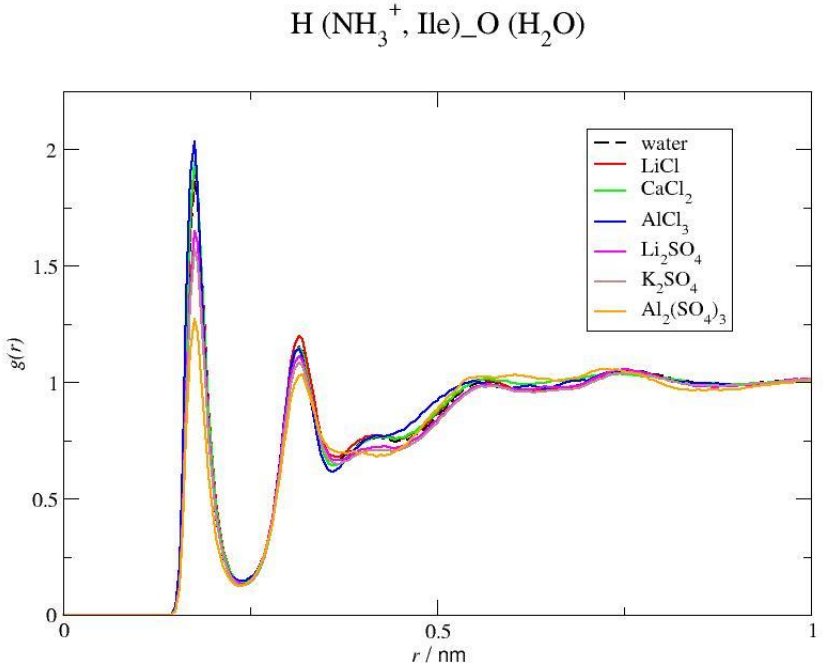

Figure 37 - Radial distribution functions corresponding to the interaction of the H atom of the amine group of isoleucine with water molecules, in the presence of all the studied salts.

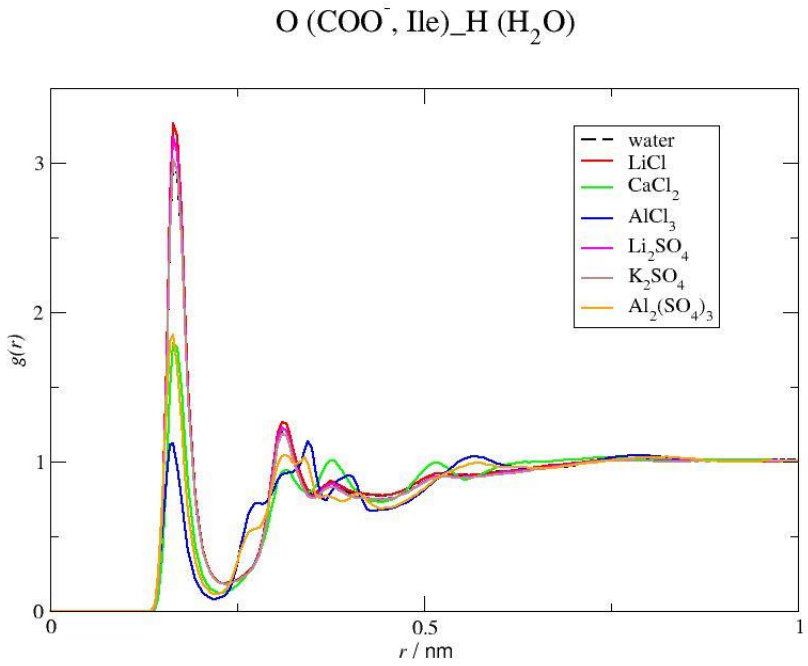

Figure 38 - Radial distribution functions corresponding to the interaction of the O atom of the carboxylic group of isoleucine with water molecules, in the presence of all the studied salts.

As shown in Figure 36, there are no significant differences in the water distribution around the terminal carbon atoms of Ile due to the presence of the different salts; however, it is possible to observe that the non-polar groups of the amino acid are less hydrated in the presence of $AlCl_3$ than in the presence of water, consistently with the discussion developed in the previous section. In the case of SO_4^{2-}salts, the amino acid has a higher hydration than in the presence of water, according to the typical behavior of a *salting-out* inducing anion.

Relatively to the charged groups of Ile, the differences in the water distribution are more significant. Analyzing the interactions of water molecules around the NH_3^+ group in Figure 37, in the presence of SO_4^{2-}, there is a decrease in the amino acid hydration while in the presence of Cl^-, the amino acid is more hydrated.

Figure 38 shows the interaction of water molecules around the carboxylic group of isoleucine. A decrease of the interactions of the carboxylic group with water is observed in the presence of the polyvalent cations whereas, in the presence of the monovalent cations, the difference is practically nonexistent. This result is consistent with the inability of the latest to

interact with COO^- and the strong affinity of the polyvalent cations with the carboxyl group pointed out above.

As discussed in the previous section, these differences in the amino acids hydration are due to the ions specific interactions with the biomolecules in the aqueous solutions.

In the Appendix A, the results obtained for alanine and valine are presented in Figures A.14-A.16 andFigures A.17-A.19, respectively. Their behavior is similar to that of isoleucine.

3.3.4. Amino acid side chain effect

To analyze the effect of the length of the amino acid side chain in the solubility effect promoted by the anions, the RDFs corresponding to the interactions between the terminal carbon atoms of the three amino acids studied and the anion of Li_2SO_4 (Figure 39) was selected, since this salt has a weakly hydrated cation with a negligible effect and an anion with a pronounced effect on the aqueous solubility of the amino acids. In the case of the cations, Figures 40 and 41 was selected, showing the RDFs corresponding to the interactions between different molecular regions of the three amino acids with the cation in $AlCl_3$ systems. Following the same reasoning, this salt was chosen because it has an anion positioned in the middle of the Hofmeister series and a strongly hydrated polyvalent cation with pronounced effect on the amino acids aqueous solubilities.

3.3.4.1. Anions

As can be observed in Figure 39, the strength of the interactions of the terminal carbon atoms with the anion decreases with the increase of the amino acid side chain. In the case of Ala and Val there is, although weak, some association to the terminal carbon atoms. In the case of Ile, the interaction with the terminal carbon atom is practically nonexistent.

This observation supports the fact that SO_4^{2-} does not favorably interact with the non-polar moieties of the amino acids, as a *salting-out* anion. The same occurs for the other salts containing SO_4^{2-}, as can be observed in the Appendix, Figures A.20 and A.21. This is supported by the experimental results. For example, Li_2SO_4 induces a more pronounced *salting-out* effect for Ile than for Val (Table 7).

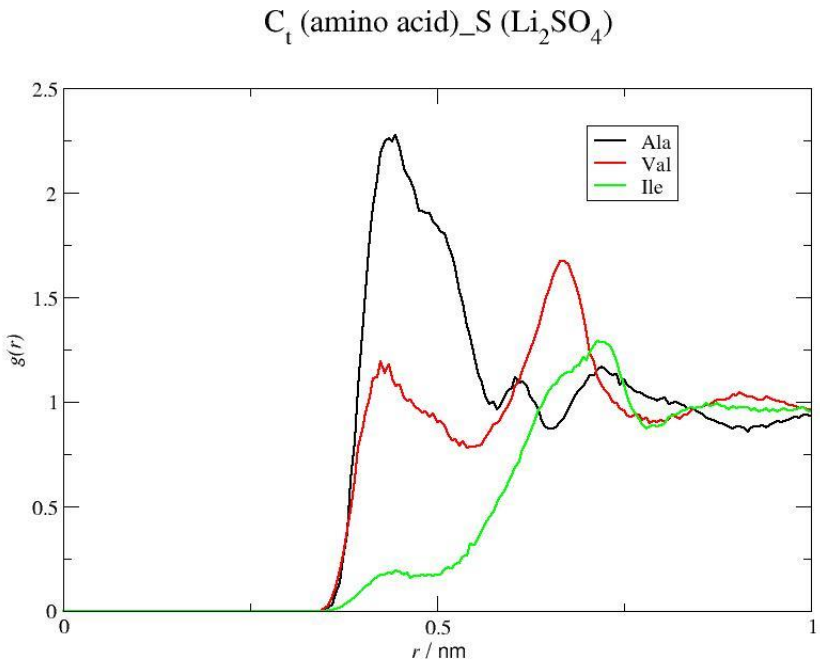

Figure 39 - Radial distribution functions corresponding to the interaction of the terminal carbon atom of all the amino acids studied with the central atom of the anion for aqueous solutions of Li_2SO_4.

3.3.4.2. Cations

In Figure 40 it is noticeable that the stronger C_t-cation interaction occurs again in the case of Ala, but this is likely to be a reflex of the affinity of the cation to the charged carboxyl group, and of the small size of this amino acid. In Figure 41, there is no specific trend. This behavior is observed as well for $CaCl_2$, a salt also containing an anion positioned in the middle of the Hofmeister series and a cation with a strong solubility effect, as can be observed in Figures A.22 and A.23. The alkyl chain length of the amino acids does not seem to significantly influence the solubility effect observed when the salt comprises a polyvalent cation, which would be expected assuming a molecular mechanism ruled by the COO^--cation interactions. These results are in good agreement with the available experimental data. As shown in Figure 18 while $CaCl_2$ induces a significant increase in the solubility of Val and Ile in water, a more pronounced increase is observed for Ala.

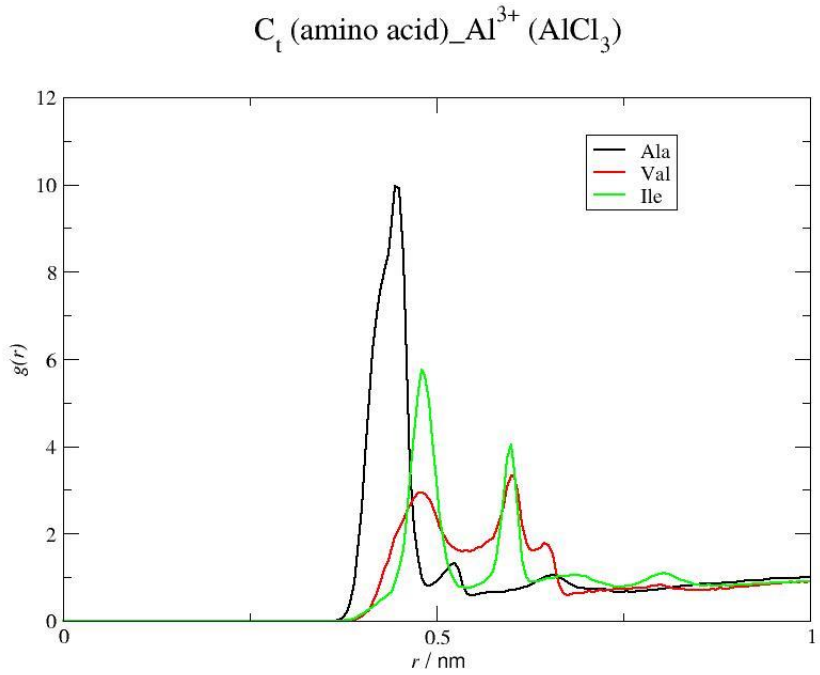

Figure 40 - Radial distribution functions corresponding to the interactions of all the studied amino acids C_t with the cation of $AlCl_3$.

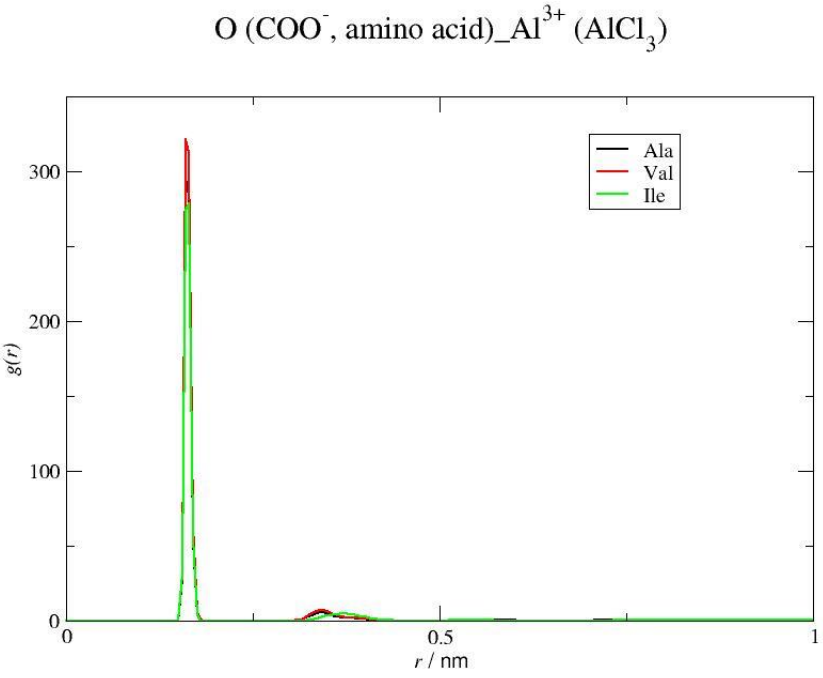

Figure 41 - Radial distribution functions corresponding to the interactions of the O atom of the carboxylic group of all the studied amino acids with the cation of $AlCl_3$.

Chapter 4. Conclusions and Future Work

New solubility data were measured, at 298.15 K, for DL-alanine in aqueous solutions of $CaCl_2$ and K_2SO_4, and for L-isoleucine and L-valine in aqueous solutions of $CaCl_2$, K_2SO_4, LiCl, Li_2SO_4, $Al_2(SO_4)_3$ and $AlCl_3$.

The molecular dynamics simulations performed suggest that SO_4^{-2} does not establish significant interactions with the non-polar moieties of the amino acids and interacts with the positively charged group, having a tipical behavior of a *salting-out* inducing agent, positioned in the extreme of the Hofmeister series. In fact, the interaction of the high charge density SO_4^{2-} anion with a hydrophobic moiety of the amino acid is a highly unfavorable process; as a consequence, this anion excludes itself from the vicinity of the non-polar groups of the amino acid. As indicated by the simulation data, the weakly hydrated Cl^- anion, positioned in the middle of the Hofmeister series, does not either establish important interactions with the non-polar parts of the amino acids, only interactions with the amino group, and will thus have less pronounced effects on the solubility, as experimentally observed for the cholride salts studied in this work.

Consistently with MD, the experimental results obtained in this work show that, in generally, LiCl, Li_2SO_4 and K_2SO_4 promote a *salting-out* effect for amino acids, being more pronounced for the last two salts.

The MD evidence gathered in this work suggests that the molecular phenomena governing the effects of *salting-in* inducing cations is different from those behind the effects of anions. Contrary to the anions, *salting-in* inducing cations do not establish important interactions with the hydrophobic parts of the amino acids, but instead with their charged parts, particularly with the carboxylic group. Strongly hydrated polyvalent cations present extremely strong interactions with the carboxylic group of the amino acids, which determine the strong *salting-in* effects observed for Ca^{2+} and Al^{3+} salts.

Relatively to the monovalent cations (Li^+ and K^+) a small effect in the amino acid solubility was observed, being smaller for Li^+ than K^+. Therefore, in these situations the effect induced by the salt will be governed by the nature of the anion.

Generally, for salts containing anions with low hydration energy and strongly hydrated cations, the magnitude of the solubility effects observed will be practically governed by the cation. In contrast, when the anion is significantly hydrated, both the cation and the anion will

have a fundamental role on the solubility of the amino acid; thus, competitive interactions will determine the amino acid solubility.

In MD simulations, the zwitterionic form of the amino acids was assumed (pH=7). However, for aluminum salts, the pH of the amino acid saline solutions is close to 2. Therefore, for these systems, it would be interesting to perform molecular dynamic simulations considering also the presence of the acid form of the amino acid.

References

Aaqvist, J. (1990). "Ion-water interaction potentials derived from free energy perturbation simulations." The Journal of Physical Chemistry **94**(21): 8021-8024.

Allen, M. P. (2004). "Introduction to Molecular Dynamics Simulation." John von Neumann Institute for Computing **23**: 1-28.

Arakawa, T. and Timasheff, S. N. (1984). "Mechanism of protein salting in and salting out by divalent cation salts: balance between hydration and salt binding." Biochemistry **23**(25): 5912-5923.

Batista, M. L. S., Tomé, L. I. N., Neves, C. M. S. S., Rocha, E. M., Gomes, J. R. B. and Coutinho, J. A. P. (2012). "The Origin of the LCST on the Liquid–Liquid Equilibrium of Thiophene with Ionic Liquids." The Journal of Physical Chemistry B **116**(20): 5985-5992.

Berendsen, H. J. C., Grigera, J. R. and Straatsma, T. P. (1987). "The missing term in effective pair potentials." The Journal of Physical Chemistry **91**(24): 6269-6271.

Brown, M. G. and Rousseau, R. W. (1994). "Effect of Sodium-Hydroxide on the Solubilities of L-Isoleucine, L-Leucine, and L-Valine." Biotechnology Progress **10**(3): 253-257.

Cannon, W. R., Pettitt, B. M. and McCammon, J. A. (1994). "Sulfate Anion in Water: Model Structural, Thermodynamic, and Dynamic Properties." The Journal of Physical Chemistry **98**(24): 6225-6230.

Chandrasekhar, J., Spellmeyer, D. C. and Jorgensen, W. L. (1984). "Energy component analysis for dilute aqueous solutions of lithium(1+), sodium(1+), fluoride(1-), and chloride(1-) ions." Journal of the American Chemical Society **106**(4): 903-910.

Collins, K. D. (2004). "Ions from the Hofmeister series and osmolytes: effects on proteins in solution and in the crystallization process." Methods **34**(3): 300-311.

Dalton, J. B. and Schmidt, C. L. A. (1933). "The solubilities of certain amino acids in water, the densities of their solutions at twenty-five degrees, and the calculated heats of solution and partial molal volumes*." Journal of Biological Chemistry **103**(2): 549-578.

Dunn, M. S., Ross, F. J. and Read, L. S. (1933). "THE SOLUBILITY OF THE AMINO ACIDS IN WATER." Journal of Biological Chemistry **103**(2): 579-595.

El-Dossoki, F. (2010). "Effect of the Charge and the Nature of Both Cations and Anions on the Solubility of Zwitterionic Amino Acids, Measurements and Modeling." Journal of Solution Chemistry **39**(9): 1311-1326.

Essmann, U., Perera, L., Berkowitz, M., Darden, T., Lee, H. and Pedersen, L. (1995). "A smooth particle mesh Ewald method." The Journal of Chemical Physics **103**(19): 8577-8593.

Fadda, E. and Woods, R. J. (2010). "Molecular simulations of carbohydrates and protein–carbohydrate interactions: motivation, issues and prospects." Drug Discovery Today **15**(15–16): 596-609.

Faro, T. M. C., Thim, G. P. and Skaf, M. S. (2010). "A Lennard-Jones plus Coulomb potential for Al3+ ions in aqueous solutions." The Journal of Chemical Physics **132**(11): 114509-114501 - 114509-114508.

Fernandes, F. M. S. S. (1988). "Simulação Computacional - O método da dinâmica molecular." Rev. Ciência **Série V**(2): 10-15.

Ferreira, L. A., Macedo, E. A. and Pinho, S. P. (2005). "Effect of KCl and Na2SO4 on the Solubility of Glycine and dl-Alanine in Water at 298.15 K." Industrial & Engineering Chemistry Research **44**(23): 8892-8898.

Ferreira, L. A., Macedo, E. A. and Pinho, S. P. (2007). "KCl effect on the solubility of five different amino acids in water." Fluid Phase Equilibria **255**(2): 131-137.

Ferreira, L. A., Macedo, E. A. and Pinho, S. P. (2009). "The effect of ammonium sulfate on the solubility of amino acids in water at (298.15 and 323.15) K." The Journal of Chemical Thermodynamics **41**(2): 193-196.

Füser, G. and Steinbüchel, A. (2005). "Investigations on the Solubility Behavior of Cyanophycin. Solubility of Cyanophycin in Solutions of Simple Inorganic Salts." Biomacromolecules **6**(3): 1367-1374.

Gekko, K. (1981). "Mechanism of Polyol-Induced Protein Stabilization - Solubility of Amino-Acids and Diglycine in Aqueous Polyol Solutions." Journal of Biochemistry **90**(6): 1633-1641.

Gekko, K. and Idota, Y. (1989). "Amino-Acid Solubility and Protein Stability in Aqueous Maltitol Solutions." Agricultural and Biological Chemistry **53**(1): 89-95.

Gekko, K., Ohmae, E., Kameyama, K. and Takagi, T. (1998). "Acetonitrile-protein interactions: amino acid solubility and preferential solvation." Biochimica Et Biophysica Acta-Protein Structure and Molecular Enzymology **1387**(1-2): 195-205.

Haile, J. M. (1997). Molecular Dynamics Simulation: Elementary Methods. New York, John Wiley.

Hess, B., Bekker, H., Berendsen, H. J. C. and Fraaije, J. G. E. M. (1997). "LINCS: A linear constraint solver for molecular simulations." Journal of Computational Chemistry **18**(12): 1463-1472.

Hess, B., Kutzner, C., van der Spoel, D. and Lindahl, E. (2008). "GROMACS 4: Algorithms for Highly Efficient, Load-Balanced, and Scalable Molecular Simulation." Journal of Chemical Theory and Computation **4**(3): 435-447.

Hockney, R. W., Goel, S. P. and Eastwood, J. W. (1974). "Quiet high-resolution computer models of a plasma." Journal of Computational Physics **14**(2): 148-158.

Hofmeister, F. (1888). "Zur Lehre von der Wirkung der Salze." Archiv für experimentelle Pathologie und Pharmakologie **24**(4-5): 247-260.

Islam, M. N. and Wadi, R. K. (2001). "Thermodynamics of Transfer of Amino Acids from Water to Aqueous Sodium Sulfate." Physics and Chemistry of Liquids **39**(1): 77-84.

Jin, X. Z. and Chao, K. C. (1992). "Solubility of four amino acids in water and of four pairs of amino acids in their water solutions." Journal of Chemical & Engineering Data **37**(2): 199-203.

Kherb, J., Flores, S. C. and Cremer, P. S. (2012). "Role of Carboxylate Side Chains in the Cation Hofmeister Series." The Journal of Physical Chemistry B **116**(25): 7389-7397.

Khoshkbarchi, M. K. and Vera, J. H. (1997). "Effect of NaCl and KCl on the Solubility of Amino Acids in Aqueous Solutions at 298.2 K: Measurements and Modeling." Industrial & Engineering Chemistry Research **36**(6): 2445-2451.

Kunz, W. (2010). "Specific ion effects in colloidal and biological systems." Current Opinion in Colloid & Interface Science **15**(1–2): 34-39.

Kunz, W., Henle, J. and Ninham, B. W. (2004). "'Zur Lehre von der Wirkung der Salze' (about the science of the effect of salts): Franz Hofmeister's historical papers." Current Opinion in Colloid & Interface Science **9**(1-2): 19-37.

Kuramochi, H., Noritomi, H., Hoshino, D. and Nagahama, K. (1996). "Measurements of solubilities of two amino acids in water and prediction by the UNIFAC model." Biotechnology Progress **12**(3): 371-379.

Lide, D. R. (2003). CRC Handbook of Chemistry and Physics, 84th Edition, Taylor & Francis.

Lund, M., Vrbka, L. and Jungwirth, P. (2008). "Specific Ion Binding to Nonpolar Surface Patches of Proteins." Journal of the American Chemical Society **130**(35): 11582-11583.

MacKerell, A. D., Bashford, D., Bellott, M., Dunbrack, R. L., Evanseck, J. D., Field, M. J., Fischer, S., Gao, J., Guo, H., Ha, S., Joseph-McCarthy, D., Kuchnir, L., Kuczera, K., Lau, F. T. K., Mattos, C., Michnick, S., Ngo, T., Nguyen, D. T., Prodhom, B., Reiher, W. E., Roux, B., Schlenkrich, M., Smith, J. C., Stote, R., Straub, J., Watanabe, M., Wiórkiewicz-Kuczera, J., Yin, D. and Karplus, M. (1998). "All-Atom Empirical Potential for Molecular Modeling and Dynamics Studies of Proteins†." The Journal of Physical Chemistry B **102**(18): 3586-3616.

Marcus, Y. (1997). Ion Properties. New York, Marcus Dekker Inc.

Matsuo, H., Suzuki, Y. and Sawamura, S. (2002). "Solubility of alpha-amino acids in water under high pressure: glycine, L-alanine, L-valine, L-leucine, and L-isoleucine." Fluid Phase Equilibria **200**(2): 227-237.

Nelson, D. L. and Cox, M. M. (2008). Lehninger principles of biochemistry. New York, Worth Publishers.

Nosé, S. (1984). "A molecular dynamics method for simulations in the canonical ensemble." Molecular Physics **52**(2): 255-268.

Orella, C. J. and Kirwan, D. J. (1991). "Correlation of Amino-Acid Solubilities in Aqueous Aliphatic Alcohol-Solutions." Industrial & Engineering Chemistry Research **30**(5): 1040-1045.

Parrinello, M. and Rahman, A. (1981). "Polymorphic transitions in single crystals: A new molecular dynamics method." Journal of Applied Physics **52**(12): 7182-7190.

Pradhan, A. A. and Vera, J. H. (1998). "Effect of acids and bases on the solubility of amino acids." Fluid Phase Equilibria **152**(1): 121-132.

Pradhan, A. A. and Vera, J. H. (2000). "Effect of anions on the solubility of zwitterionic amino acids." Journal of Chemical and Engineering Data **45**(1): 140-143.

Ramasami, P. (2002). "Solubilities of Amino Acids in Water and Aqueous Sodium Sulfate and Related Apparent Transfer Properties." Journal of Chemical & Engineering Data **47**(5): 1164-1166.

Rapaport, D. C. (2004). The Art of Molecular Dynamics Simulation, Cambridge University Press.

Sasahara, K. and Uedaira, H. (1993). "Solubility of Amino-Acids in Aqueous Poly(Ethylene Glycol) Solutions." Colloid and Polymer Science **271**(11): 1035-1041.

Smith, D. E. and Dang, L. X. (1994). "Computer simulations of NaCl association in polarizable water." The Journal of Chemical Physics **100**(5): 3757-3766.

Teja, A. S., Givand, J. C. and Rousseau, R. W. (2002). "Correlation and prediction of crystal solubility and purity." Aiche Journal **48**(11): 2629-2634.

Tian, J., Yin, Y., Sun, H. and Luo, X. (2002). "Magnesium chloride: an efficient 13C NMR relaxation agent for amino acids and some carboxylic acids." Journal of Magnetic Resonance **159**(2): 137-144.

Tomé, L. I. N., Jorge, M., Gomes, J. R. B. and Coutinho, J. A. P. (2012). "Molecular Dynamics Simulation Studies of the Interactions between Ionic Liquids and Amino Acids in Aqueous Solution." The Journal of Physical Chemistry B **116**(6): 1831-1842.

Tomé, L. I. N., Jorge, M., Gomes, J. R. B. and Coutinho, J. A. P. (2010). "Toward an Understanding of the Aqueous Solubility of Amino Acids in the Presence of Salts: A Molecular Dynamics Simulation Study." The Journal of Physical Chemistry B **114**(49): 16450-16459.

Tomé, L. I. N., Pinho, S. P., Jorge, M., Gomes, J. R. B. and Coutinho, J. A. P. (2013). "Salting-in with a Salting-out Agent: Explaining the Cation Specific Effects on the Aqueous Solubility of Amino Acids." The Journal of Physical Chemistry B **117**(20): 6116-6128.

Venkatesu, P., Lee, M. J. and Lin, H. M. (2006). "Transfer free energies of peptide backbone unit from water to aqueous electrolyte solutions at 298.15 K." Biochemical Engineering Journal **32**(3): 157-170.

Weerasinghe, S. and Smith, P. E. (2003). "A Kirkwood–Buff derived force field for sodium chloride in water." The Journal of Chemical Physics **119**(21): 11342-11349.

Xie, W. J. and Gao, Y. Q. (2013). "A Simple Theory for the Hofmeister Series." The Journal of Physical Chemistry Letters **4**(24): 4247-4252.

Yoo, J. and Aksimentiev, A. (2011). "Improved Parametrization of Li^+, Na^+, K^+, and Mg^{2+} Ions for All-Atom Molecular Dynamics Simulations of Nucleic Acid Systems." The Journal of Physical Chemistry Letters **3**(1): 45-50.

Zhang, Y., Furyk, S., Bergbreiter, D. E. and Cremer, P. S. (2005). "Specific Ion Effects on the Water Solubility of Macromolecules: PNIPAM and the Hofmeister Series." Journal of the American Chemical Society **127**(41): 14505-14510.

Zumstein, R. C. and Rousseau, R. W. (1989). "Solubility of L-Isoleucine in and Recovery of L-Isoleucine from Neutral and Acidic Aqueous-Solutions." Industrial & Engineering Chemistry Research **28**(8): 1226-1231.

Appendix A

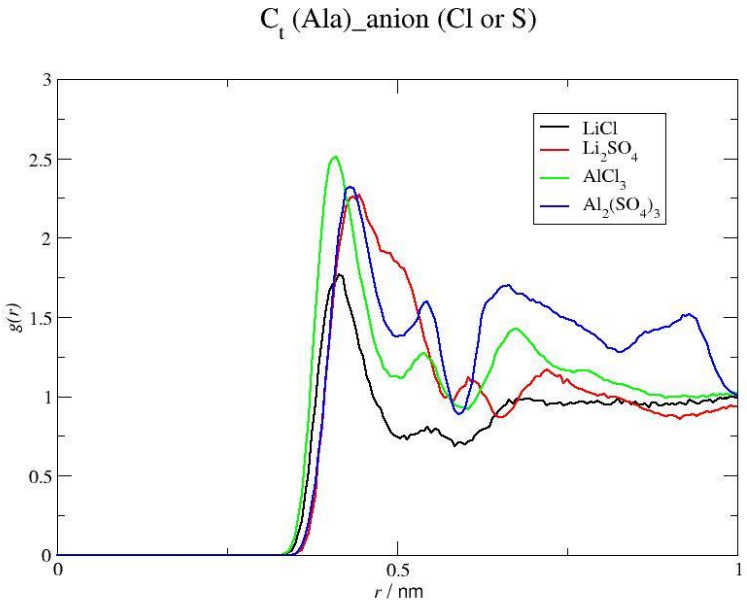

Figure A.1 - Radial distribution functions corresponding to the interactions of alanine C_t with the central atom of the anions (Cl or S), for salts containing Li^+ and Al^{3+} cations.

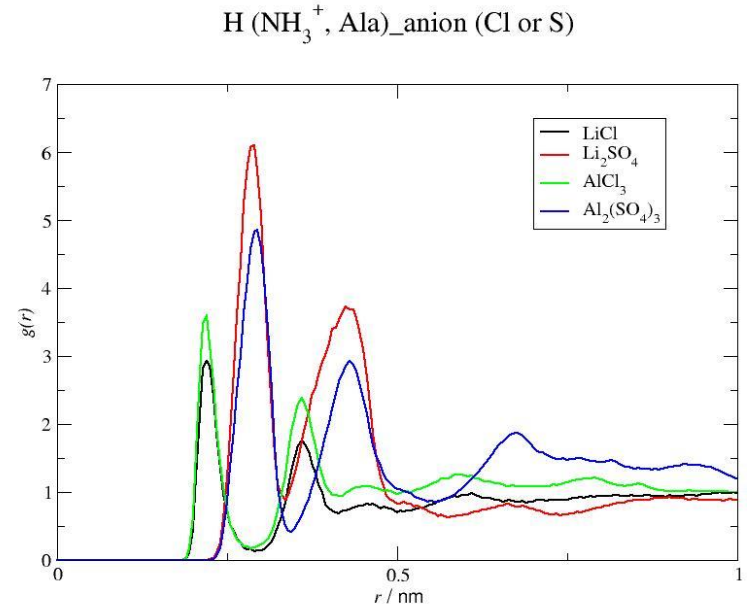

Figure A.2 - Radial distribution functions corresponding to the interactions of the H atom of the amine group of alanine with the central atom of the anions (Cl or S), for salts containing Li^+ and Al^{3+} cations.

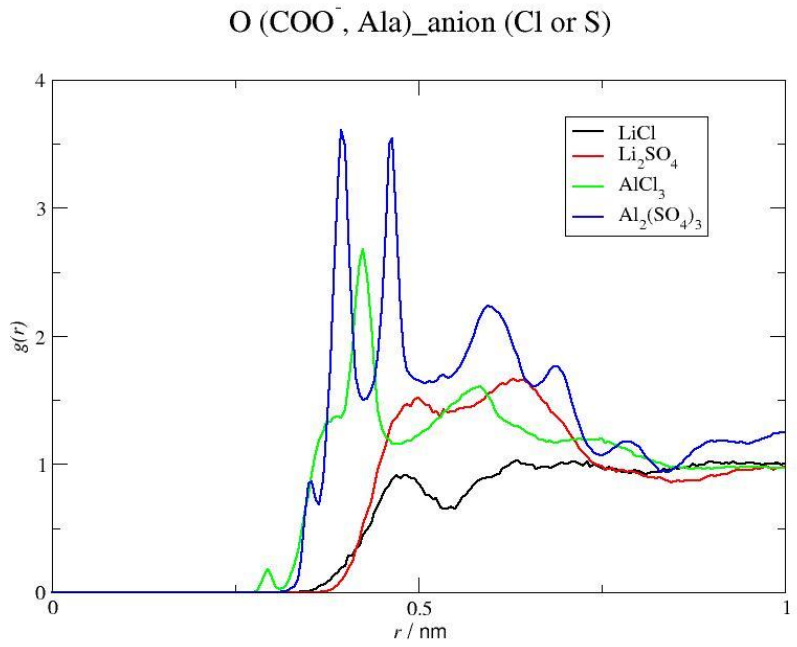

Figure A.3 - Radial distribution functions corresponding to the interactions of the O atom of the carboxylic group of alanine with the central atom of the anions (Cl or S), for salts containing Li^+ and Al^{3+} cations.

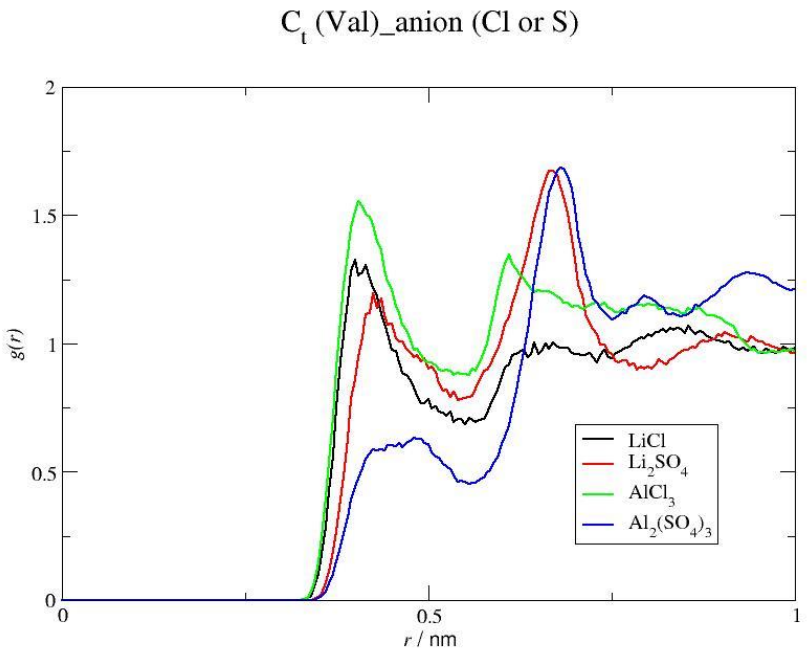

Figure A.4 - Radial distribution functions corresponding to the interactions of valine C_t with the central atom of the anions (Cl or S), for salts containing Li^+ and Al^{3+} cations.

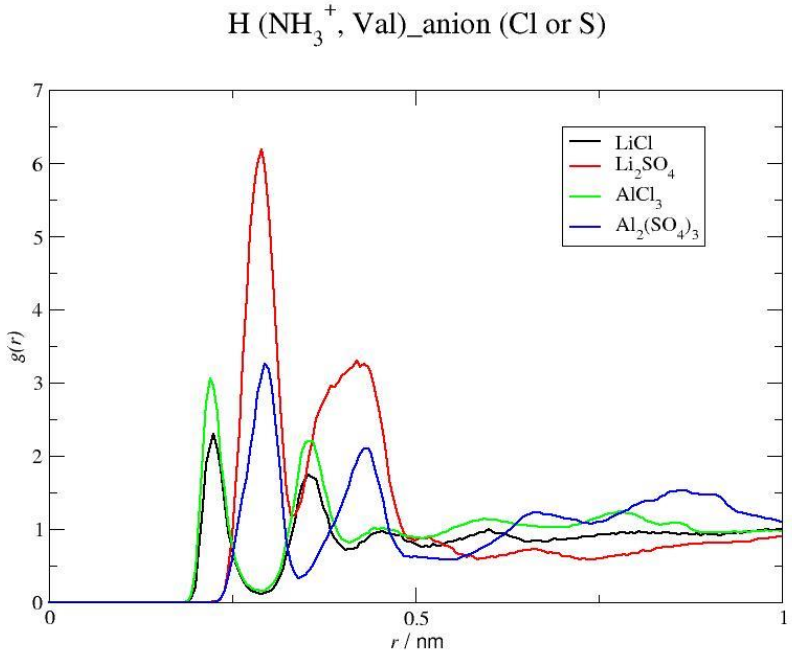

Figure A.5 - Radial distribution functions corresponding to the interactions of the H atom of the amine group of valine with the central atom of the anions (Cl or S), for salts containing Li^+ and Al^{3+} cations.

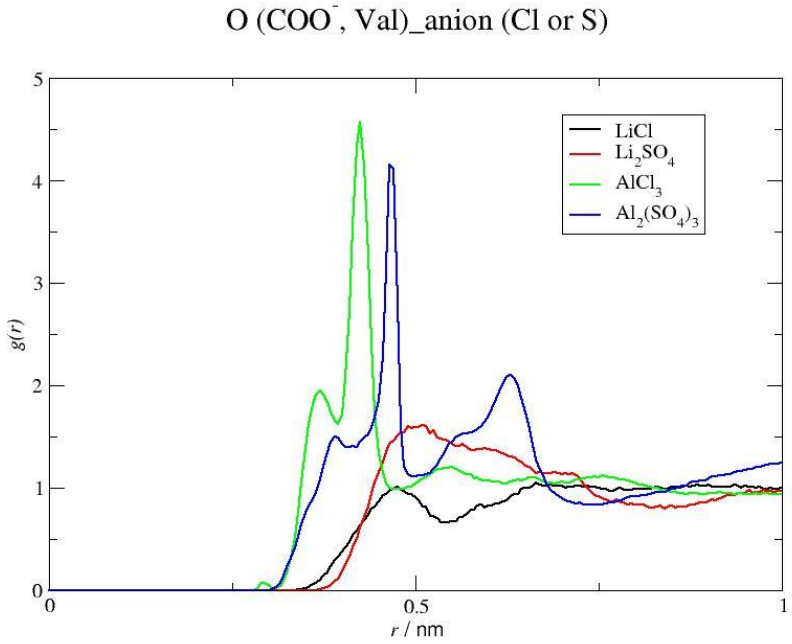

Figure A.6 - Radial distribution functions corresponding to the interactions of the O atom of the carboxylic group of valine with the central atom of the anions (Cl or S), for salts containing Li^+ and Al^{3+} cations.

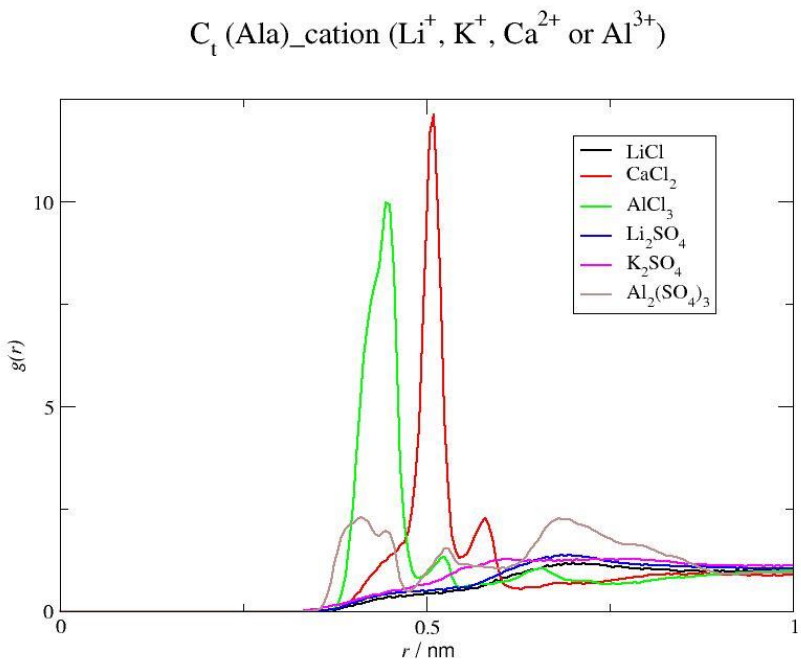

Figure A.7 - Radial distribution functions corresponding to the interactions of alanine Ct with the cations (Li^+, K^+, Ca^{2+} or Al^{3+}) for all the studied salts.

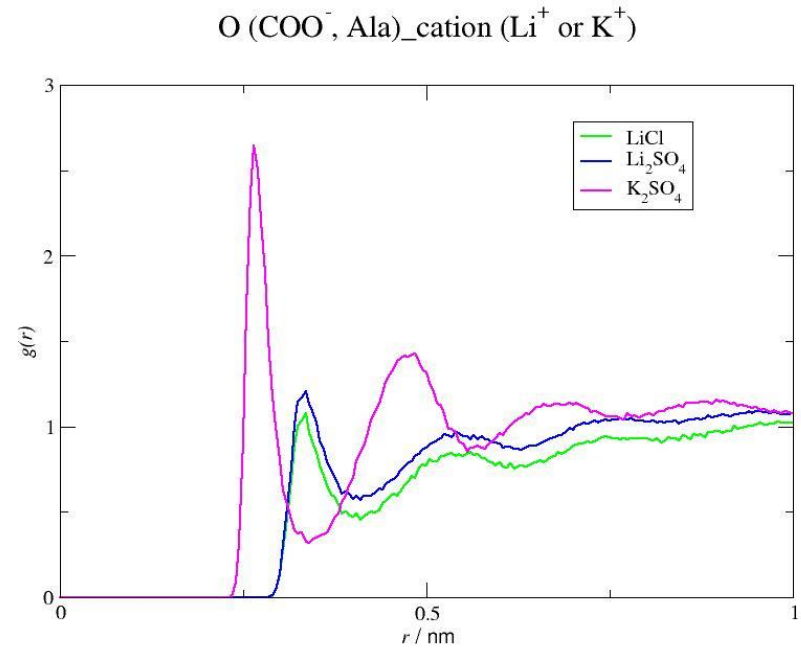

Figure A.8 - Radial distribution functions corresponding to the interactions of the O atom of the carboxylic group of alanine with the monovalent cations (Li^+ or K^+) for all the studied salts.

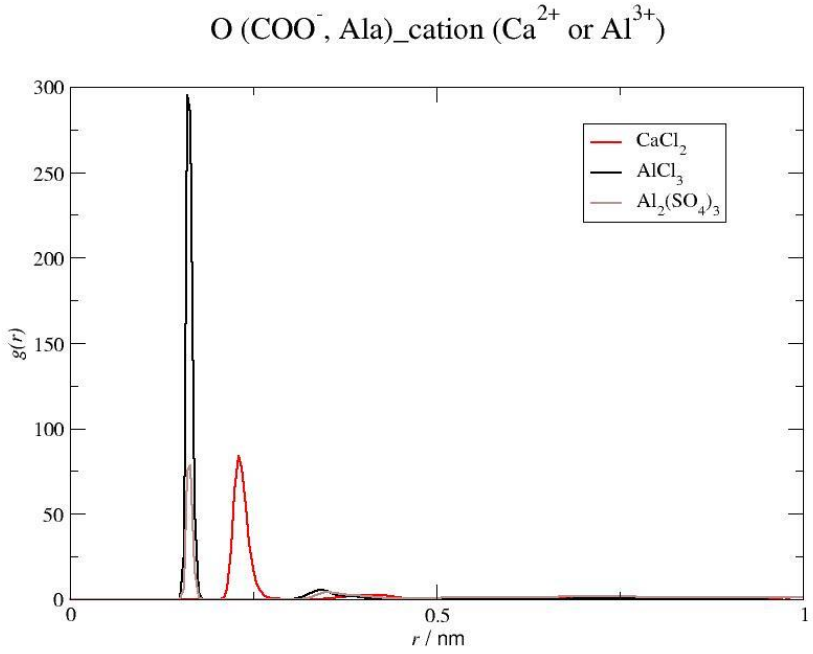

Figure A.9 - Radial distribution functions corresponding to the interactions of the O atom of the carboxylic group of alanine with the polyvalent cations (Ca^{2+} or Al^{3+}) for all the studied salts.

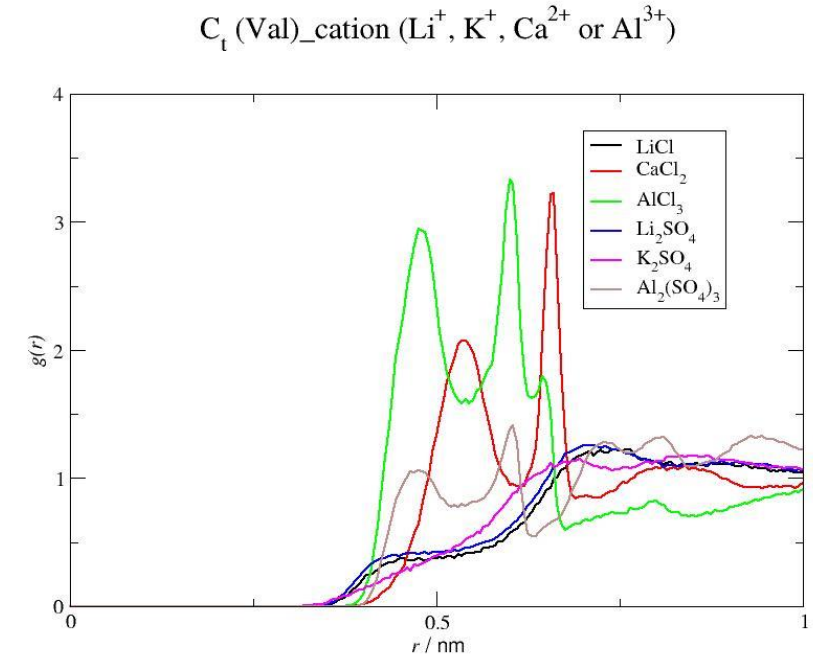

Figure A.10 - Radial distribution functions corresponding to the interactions of valine C_t with the cations (Li^+, K^+, Ca^{2+} or Al^{3+}) for all the studied salts.

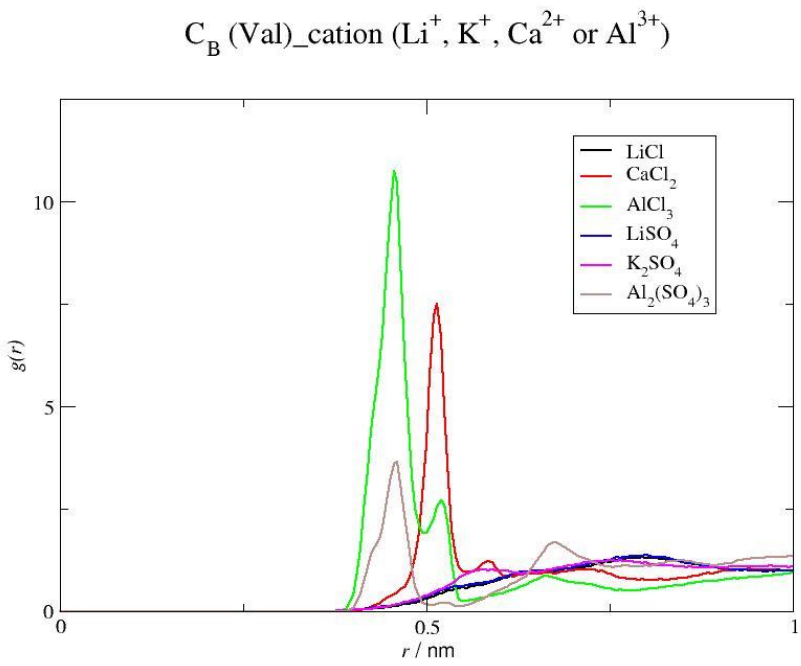

Figure A.11 - Radial distribution functions corresponding to the interactions of valine C_B with the cations (Li^+, K^+, Ca^{2+} or Al^{3+}) for all the studied salts.

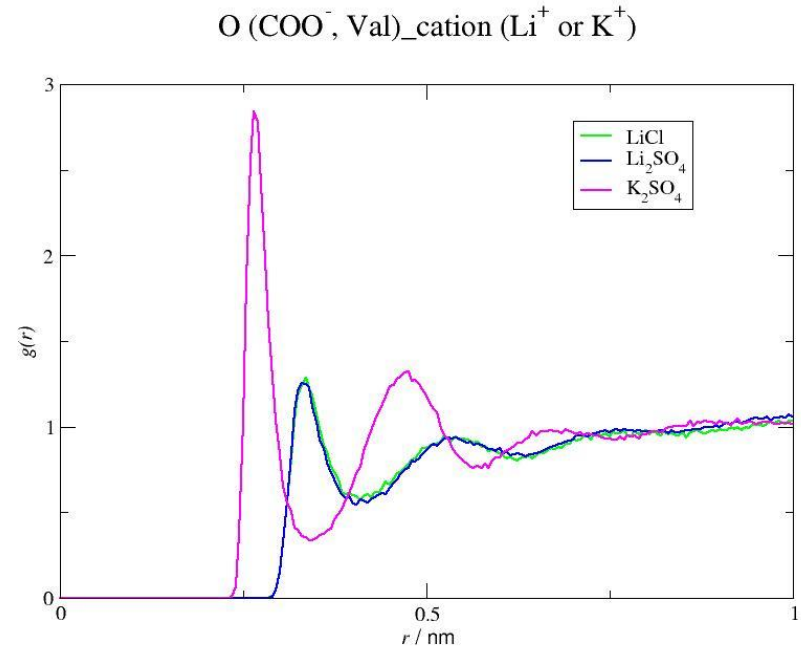

Figure A.12 - Radial distribution functions corresponding to the interactions of the O atom of the carboxylic group of valine with the monovalent cations (Li^+ or K^+) for all the studied salts.

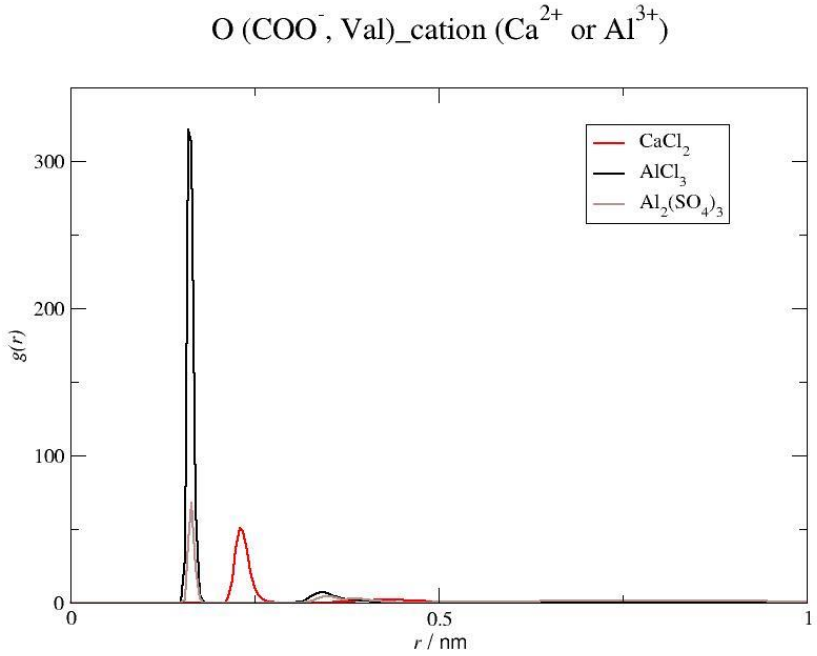

Figure A.13 - Radial distribution functions corresponding to the interactions of the O atom of the carboxylic group of valine with the polyvalent cations (Ca^{2+} or Al^{3+}) for all the studied salts.

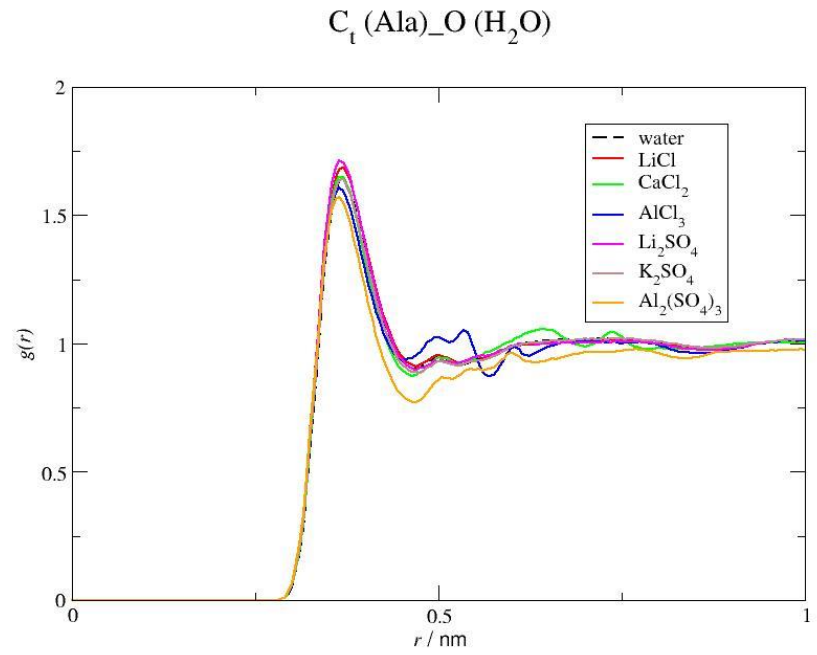

Figure A.14 - Radial distribution functions corresponding to the interaction of alanine C_t with water molecules, in the presence of all the studied salts.

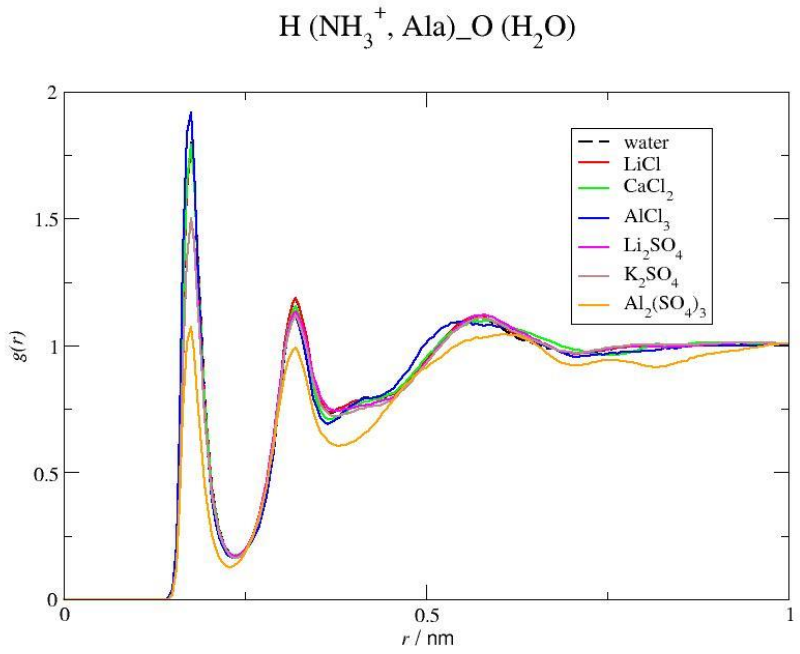

Figure A.15 - Radial distribution functions corresponding to the interaction of the H atom of the amine group of alanine with water molecules, in the presence of all the studied salts.

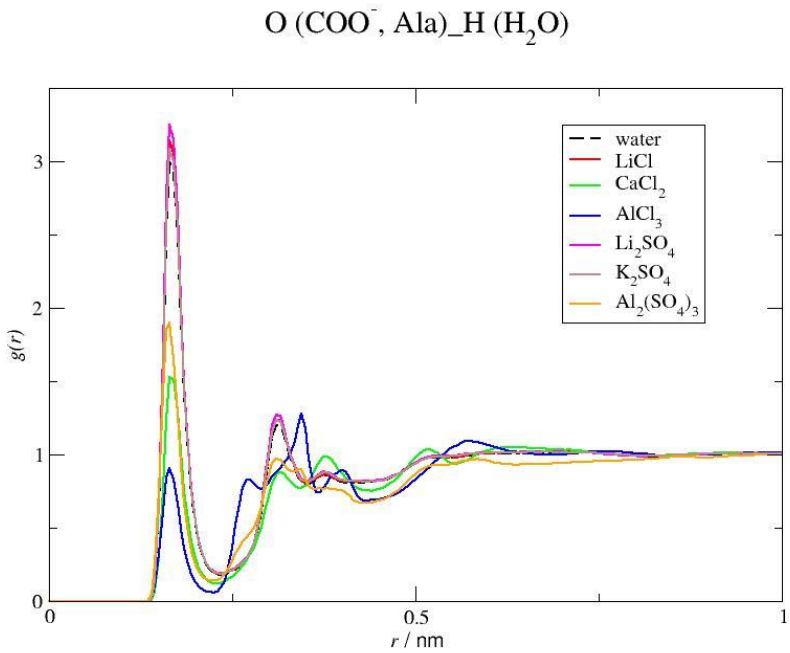

Figure A.16 - Radial distribution functions corresponding to the interaction of the O atom of the carboxylic group of alanine with water molecules, in the presence of all the studied salts.

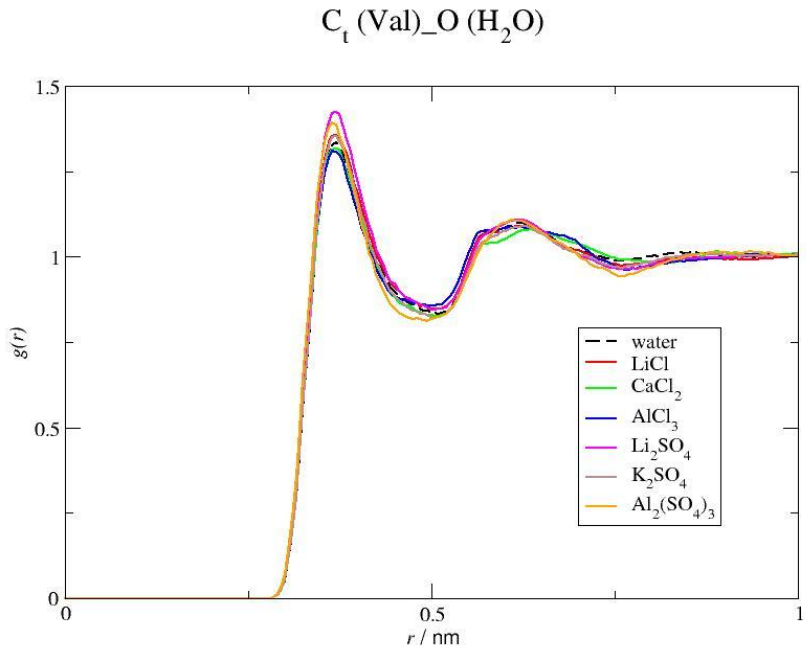

Figure A.17 - Radial distribution functions corresponding to the interaction of valine C_t with water molecules, in the presence of all the studied salts.

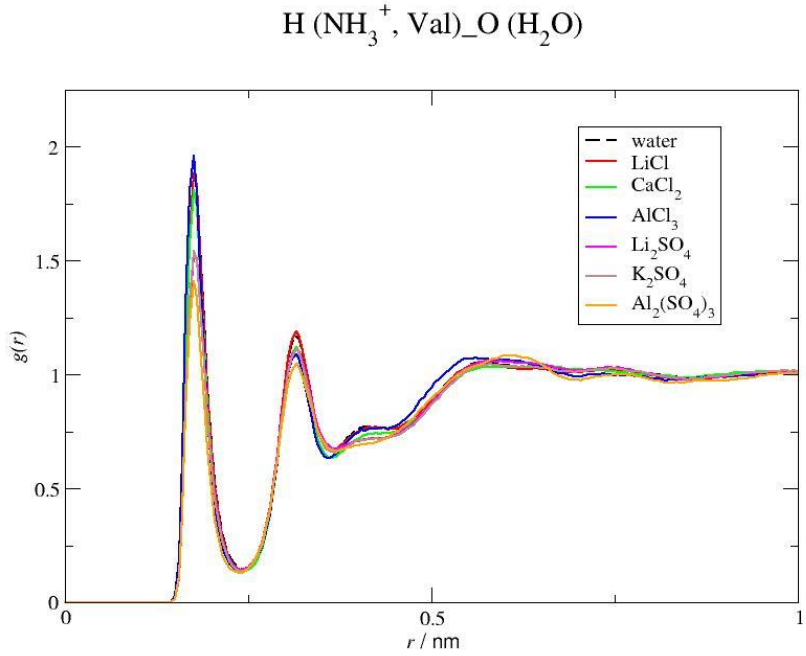

Figure A.18 - Radial distribution functions corresponding to the interaction of the H atom of the amine group of valine with water molecules, in the presence of all the studied salts.

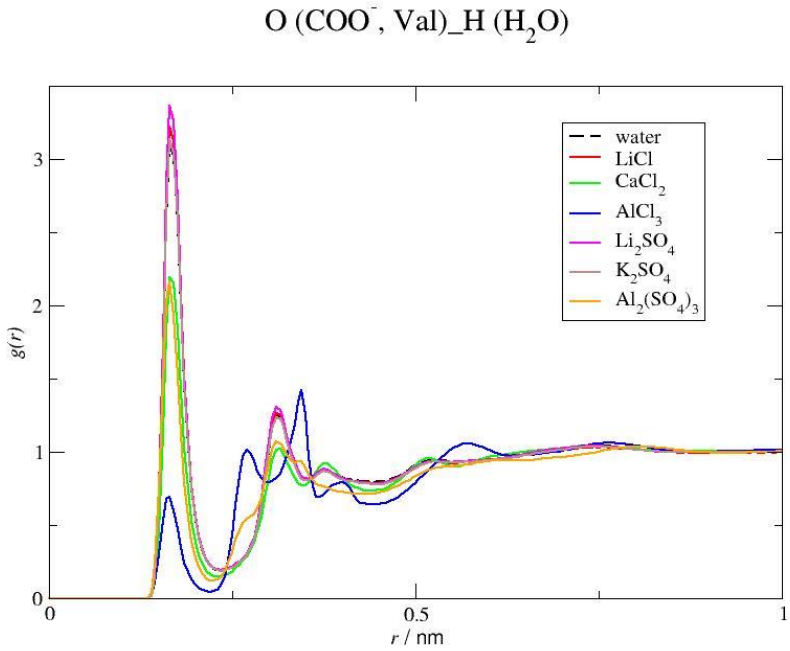

Figure A.19 - Radial distribution functions corresponding to the interaction of the O atom of the carboxylic group of valine with water molecules, in the presence of all the studied salts.

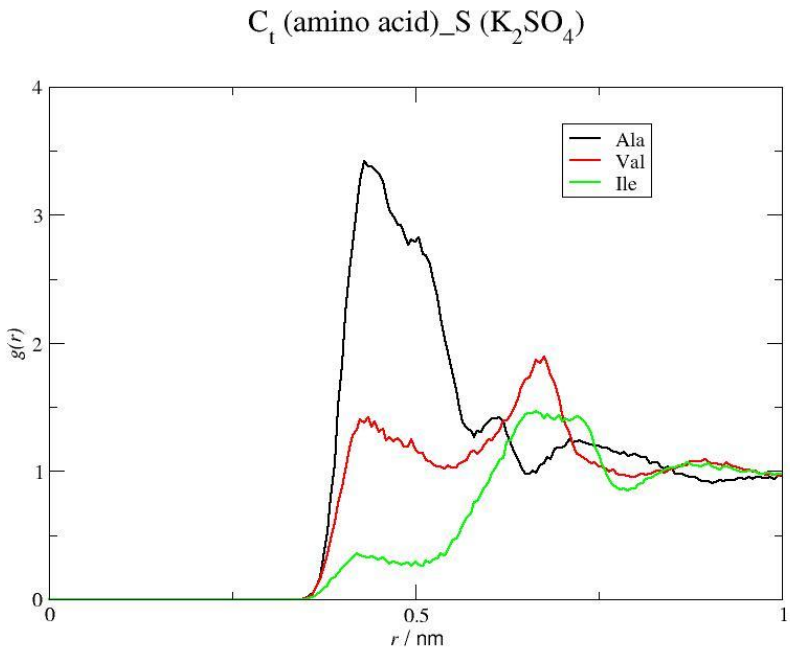

Figure A.20 - Radial distribution functions corresponding to the interaction of the terminal carbon atom of all the amino acids studied with the central atom of the anion for aqueous solutions of K_2SO_4.

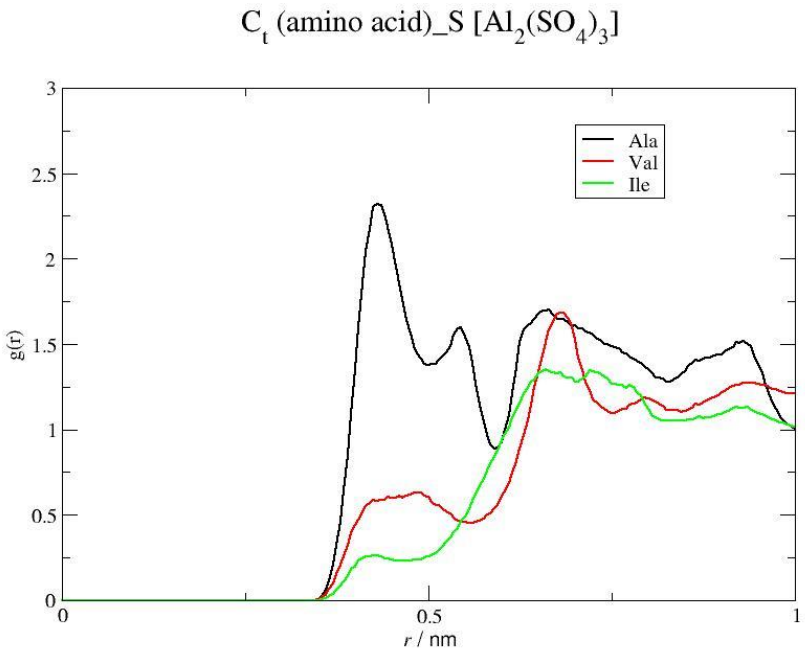

Figure A.21 - Radial distribution functions corresponding to the interaction of the terminal carbon atom of all the amino acids studied with the central atom of the anion for aqueous solutions of $Al_2(SO_4)_3$.

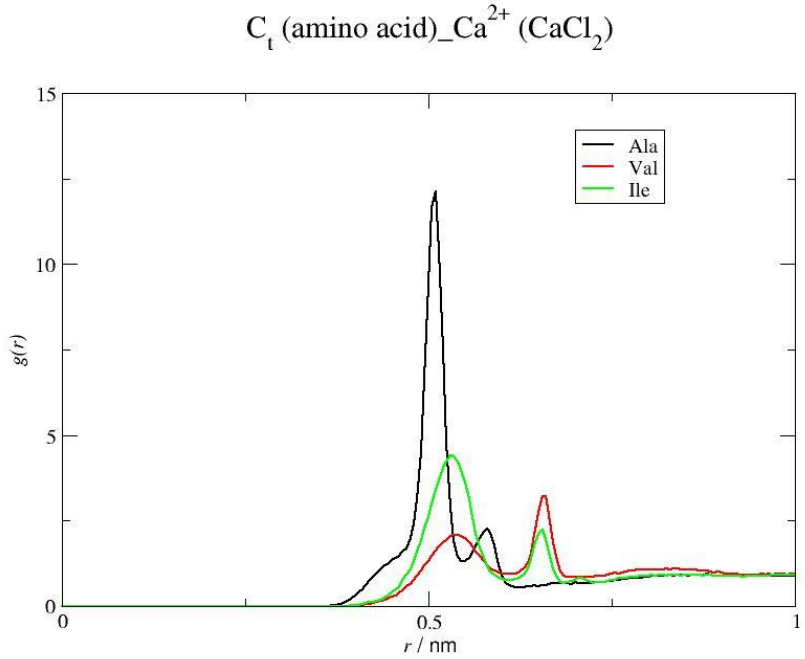

Figure A.22 - Radial distribution functions corresponding to the interactions of all the studied amino acids C_t with the cation of $CaCl_2$.

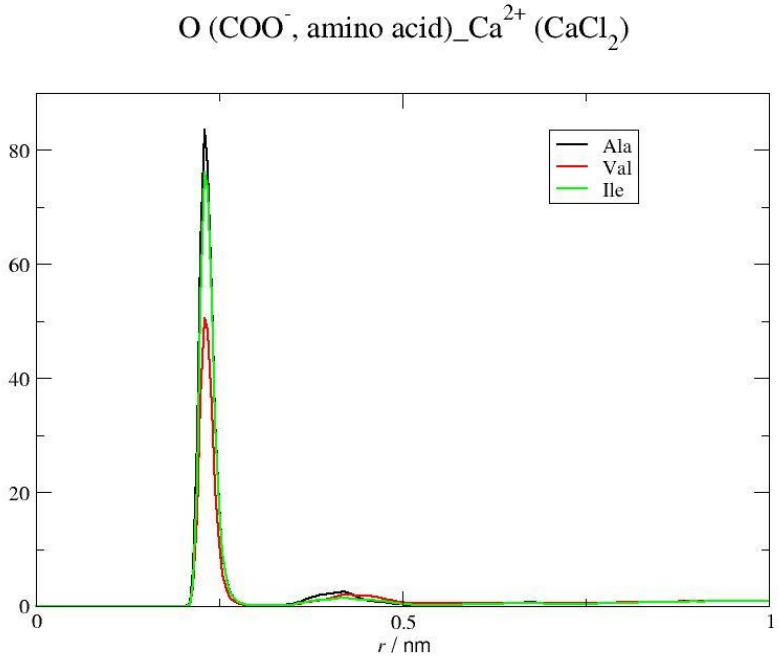

Figure A.23 - Radial distribution functions corresponding to the interactions of the O atom of the carboxylic group of all the studied amino acids with the cation of $CaCl_2$.

Table A.1 - Position and intensities of the RDF peak maxima corresponding to the interactions of selected group of Ile with the anion (A^{x-}), the cation (B^{y+}), and the oxygen (O_{H2O}) and hydrogen atoms of water (H_{H2O}), for all the systems studied.

	Water		LiCl		Li_2SO_4		$CaCl_2$		K_2SO_4		$AlCl_3$		$Al_2(SO_4)_3$	
	r/nm	g(r)	r/nm	g(r)	r/nm	g(r)	r/nm	g(r)	r/nm	g(r)	r/nm	g(r)	r/nm	g(r)
C_t - A^{x-}	-	-	-	-	0,720	1,280	0,680	1,147	0,668	1,455	0,416	1,252	0,662	1,343
H_{NH3+} - A^{x-}	-	-	0,221	1,882	0,287	3,821	0,222	3,015	0,296	6,172	0,220	2,871	0,303	4,435
			0,357	1,070	0,415	2,161	0,357	1,832	0,425	2,949	0,354	1,794	0,416	2,062
C_t - O_{H2O}	0,376	1,175	0,376	1,224	0,374	1,249	0,379	1,175	0,379	1,179	0,374	1,140	0,374	1,277
	0,624	1,098	0,624	1,112	0,624	1,109	0,631	1,126	0,629	1,088	0,646	1,095	0,619	1,140
C_t - B^{y+}	-	-	-	-	-	-	0,533	4,400	-	-	0,482	5,731	0,494	2,020
							0,658	2,220			0,602	4,019		
O_{COO} - B^{y+}	-	-	0,332	0,989	0,335	0,937	0,231	75,574	0,271	2,178	0,166	217,101	0,165	97,094
									0,475	1,153				
O_{COO} - H_{H2O}	0,167	2,987	0,166	3,247	0,166	3,141	0,171	1,788	0,168	3,001	0,168	1,109	0,173	1,840
	0,312	1,188	0,310	1,251	0,311	1,209			0,313	1,160	0,350	1,130		